Journal of Naval Architecture and Marine Engineering
June, 2020
http://dx.doi.org/10.3329/jname.v17i1.42001 http://www.banglajol.info

EFFECT OF POROUS BAFFLE ON SLOSHING PRESSURE DISTRIBUTION IN A BARGE MOUNTED CONTAINER SUBJECTED TO REGULAR WAVE EXCITATION

T. Nasar[1], S. A. Sannasiraj[2] and V. Sundar[2]

[1]Associate Professor, Department of Water Resources and Ocean Engineering, National Institute of Technology Karnataka, Surathkal, Mangalore-575025, India, Email: t.nasar@gmail.com, t.nasar@nitk.edu.in

[2]Professor, Department of Ocean Engineering, Indian Institute of Technology Madras, Chennai-600036, India, Email: sasraj@iitm.ac.in, vsundar@iitm.ac.in,

Abstract:

An experimental study has been carried out to assess the sloshing pressure expected on the side walls of the tank and on top panel. A liquid fill level with an aspect ratio (h_s /l, where h_s is the static liquid depth and l is the tank length) of 0.488 is considered which corresponds to 75% liquid fill level. In view of suppressing sloshing oscillation and consequent sloshing pressure, the baffle wall configurations such as porous wall at l/2 and porous walls at l/3 and 2l/3 were adopted. Three porosities of 15%, 20.2%, and 25.2% were considered. The sloshing tank is fitted into the freely floating barge of model scale 1:43. The barge is kept inside the wave flume in the beam sea conditions. The effects of wave excitation frequencies and on the sloshing pressure variation have been studied in detail. For comparison purpose, solid wall placed at l/2 (Nasar and Sannasiraj, 2018) is also considered and, the salient results are herein reported.

Keywords: Regular wave, barge response, sloshing pressure, porous wall, impact pressure

1. Introduction

The static-free surface in a partially filled liquid tank while subjected to external excitation extracts energy and leads to disturbance of the free surface. Thus, the free surface oscillation is called as sloshing. Impact pressure and global forces are two interests which play a major role in the design of liquid cargo ships. The magnitude of sloshing and the resulting forces on the tank walls are large when the frequency of the motion of the tank is closer to one of the natural frequencies of the sloshing liquid. If the momentum due to liquid motion is high then it may leads to capsizing of ship as well as local structural failure of containment. The resonance sloshing would occur, if, wave contains the frequency content of corresponding partial filled condition even if the ship does not experience extreme motions.

Considerable studies have been carried out on the phenomena of liquid sloshing in the late eighties. A few of the important contribution relevant to the present topic are herein discussed. Nakayama and Washizu (1980) developed finite element formulation and predicted the sloshing pressure in a container subjected to pitching oscillations. Mikelis and Journee (1984) examined the sloshing pressure in a scaled down LNG tank. Armenio and La Rocca (1996) investigated sloshing oscillation behaviour in a roll excited tank by both experimental and numerical approaches. Cariou and Casella (1999) reviewed the state of the art codes available to predict sloshing oscillation and consequent sloshing pressure. The authors emphasized the necessity of further development in the numerical approaches to predict impact loads and peak pressures. Kim (2001) discussed the simulation of sloshing flows and impact load on top panel in 2-D and 3-D tanks using finite difference algorithm. Nielsen and Mayer (2004) studied green water incidents and predicted impact pressure on the ceiling using Volume Of Fluid (VOF) method and it was validated using experimental results. Virella *et al*. (2008) studied sloshing modes and pressure distribution in rectangular tanks using linear and non-linear finite element models. Celebi and Akyildiz (2002) solved Navier Stokes equation using finite difference method and investigated the liquid sloshing in a 2-D moving tank. Akyildiz and Ünal (2005,2006) compared the observed experimental pressure distribution in a roll excited tank with the predicted pressure time traces. Bulian *et al.* (2014) conducted series of experiments subjected to roll excitation and checked the repeatability/practical ergodicity of the impact pressure on the top panel by the statistical parameters. Lu *et al.* (2015) developed viscous model and explored the vorticity and consequent damping characteristics of the horizontal baffle in a sway excited rectangular tank. Saghi (2016) developed a numerical model using coupled boundary element methods to determine pressure distribution on

1813-8535 (Print), 2070-8998 (Online) Received on: June 2019

the rectangular and trapezoidal storage tanks. Graczyk *et al.* (2006) used statistical approach on experimental data to determine the extreme value of sloshing pressure for structural designing of ships. Effect of ship headings on sloshing has been studied including beam sea condition, which induces severe sloshing load on the liquid containment. Paik and Shin (2006) developed a closed form design formulation for predicting liquid sloshing impact in a ship structure. The above said studies dealt either translational or rotational degree of excitation. Studies have also been carried out to estimate liquid sloshing pressure on its containment in the combined mode of excitations. A computational study by Akyildiz and Celebi (2002) traced the pressure time history on a tank wall subjected to combined heave and roll excitations. Bunnik and Huijsmans (2007) conducted an experimental work on a large LNG tank to estimate a sloshing impact subjected to combined sway and roll. It is to be mentioned that the results from the above said studies cannot directly be applied to the liquid containment in a floating vessel which responds to marine environment subjected to six degrees of excitations as claimed by Chen and Chiang (2000). Hence, there is a necessity to incorporate as many as possible degrees of excitation in the analytical, numerical and experimental approaches. Studies have been carried out to explore the importance of the interaction between ship motions and sloshing flows in liquid-filled tanks (Francescutto and Contento, 1994, Rognebakke and Faltinsen, 2001, Molin *et al.,* 2002, Kim *et al*., 2003, Lee *et al*., 2005, Lee *et al.,* 2007, Kim *et al.,* 2007, Nasar *et al*., 2010). As reported in the literature, the unexceptional free surface behaviour in a partially filled tank and the resulting sloshing pressure on the side walls of tank and top panel of containment expected to be severe in its life service for the combined degrees of excitations. Nasar *et al*. (2008, 2009) carried out an experimental work and discussed wave induced sloshing pressure / impact pressure.

In view of suppressing the sloshing energy/improving the damping characteristics, authors have proposed anti-slosh devices such as bottom fixed wedge shaped obstacles or sloping bottom (Modi and Akinturk, 2002), solid blocks (Modi and Munshi, 1998), submerged nets/ poles (Warnitchai and Pinkaew, 1998), floating baffles, slat screens (Tait *et al.,* 2005) and slotted screens (Crowley and Porter, 2012, Morsy *et al*., 2008, Molin and Remy 2013) etc. A numerical study by Armenio and La Rocca (1996) reported the effect of the bottom mounted solid baffle in reducing the sloshing load. Kim(2001) explored the combined effectiveness of vertical baffle and side wall stringers. Panigrahy *et al* (2009) experiment the combination of horizontal and vertical baffle to attenuate the sloshing pressure in a sway excited tank. Xue *et al.* (2012) simulated the sloshing behaviour and traced the pressure in a surge excited cubic tank. The effectiveness of different baffle wall configurations such as horizontal baffle, perforated vertical baffle, and their combinations are discussed and the results are compared with experimental data. Akyildiz (2012) used VOF technique to simulate the effect of vertical baffle height in the pitch excited two dimensional rectangular tank. The side wall pressure distribution and roof impact for the different filling condition is discussed and results are compared with experimental work.

Xue *et al.* (2017) investigated the effectiveness of the vertical baffles in suppressing the sloshing pressure in a horizontally excited tank. Four configurations such as submerged solid baffle, surface piercing baffle, surface flush baffle and porous baffle are considered. It is concluded that the porous baffle gives better results in reducing side wall impact pressure. Iranmanesh (2017) proposed a numerical model based on VOF technique and discussed the potentiality of the constrained surface floating and submerged cylinder in suppressing sloshing pressure. Cho *et al.* (2017) examined the effect of horizontal baffle wall in reducing sloshing energy and sloshing pressure on the tank walls in a sway excited tank. Boundary Element equations were developed for different porous wall conditions to compare with the experimental results. Kim *et al.* (2018) recorded the sloshing pressure in the side wall of the sway excited tank and compared with the time traces obtained for the same tank equipped with moving baffle. Chu *et al.* (2018) discussed the effect of submerged bottom mounted vertical baffles on sloshing force experienced by the sway excited sloshing tank.

Although there are considerable numerical/analytical models are reported in the literature, experimental procedures are more preferred to study the sloshing dynamics and calculation of pressure on tank walls as well as impact on tank ceiling. Further, the theoretical models are inefficient in predicting the unusual behaviour in the free surface, hydraulic jump, roof impact etc. In addition, experimental work is rather suited to study the damping characteristics of baffle in which vorticity involves. By considering the importance of combined excitations and interaction study, a freely floating barge with a rectangular tank fixed in it is allowed to oscillate in three degrees of freedom, namely, sway, heave and roll. The present paper aims to explore the characteristics of the wave induced liquid sloshing pressure on the walls of a rectangular tank and the efficacy of different porous baffle configurations in suppressing the sloshing pressure.

2. Experimental Investigations

2.1 Model details

A rectangular floating barge of breadth (B) 1.32 m and 0.65 m (D) deep was fabricated using fiber reinforced plastic. The length of the barge was 1.95 m to place across the wave flume such that beam sea test conditions were reproduced in the wave flume. A rectangular tank of size, 1.0 m (l) x 0.40 m (b) x 0.65 m (h) was also fabricated using the acrylic plate of thickness 12 mm. The longitudinal axis of the sloshing tank was oriented along the transverse width of the barge. The liquid tank was positioned inside the barge such that during the beam sea conditions, the sloshing oscillations occurred along the longitudinal axis of the tank. The liquid used for the present study is potable water. A view of the sloshing tank rigidly fixed inside a floating barge is shown in Fig. 1.

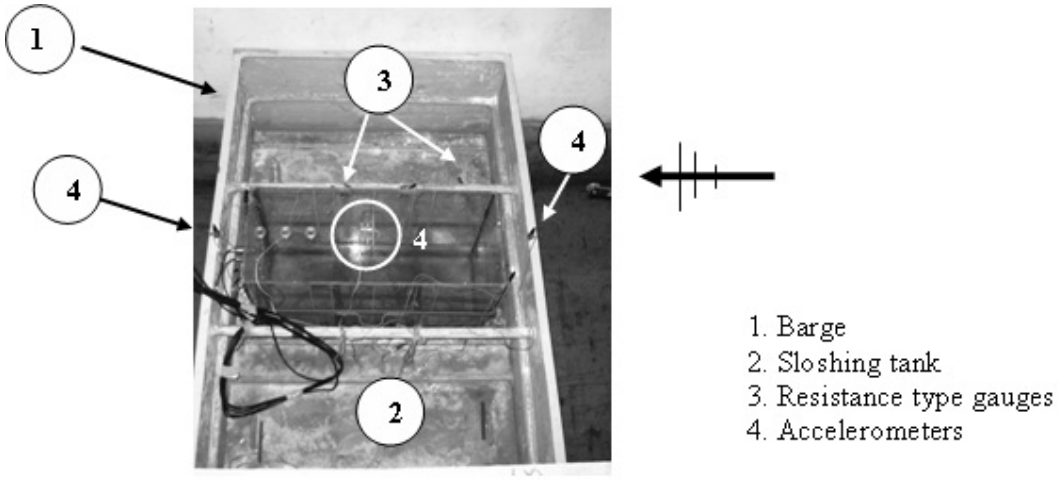

Fig. 1: View of sloshing tank fitted inside a barge in the wave flume.

2.2 Laboratory facilities and experimental procedures

The tests were conducted in a wave flume of length 50 m, width 2 m and depth 2.7 m in the department of Ocean Engineering, IIT Madras, India. The wave maker can be operated both in a piston and hinged modes, controlled by a hydraulic servo actuator. For the present study, the water depth, d was maintained as 1.0 m and the wave maker operated in the piston mode. The model was placed at a distance of 34 m from the mean position of the wave paddle. Wave probes were placed at two appropriate locations in front of the structure to trace the wave field. In addition, a wave gauge positioned on the lee side of the structure measured the transmitted wave elevation. The barge model position and the wave probe locations in the flume are shown in Fig. 2. Three inductive single axis HBM accelerometers with a measuring range of up to 100 Hz were firmly fixed on the barge model to trace the sway, heave, and roll response time histories due to the combined wave action and sloshing. The sloshing tank was instrumented on its walls with four resistive gauges to trace the liquid oscillation. Strain gauge type pressure transducers (P1-P5, KISTLER RTC 28) with a measuring range of up to 0.2 bar were fixed on the vertical side of the tank with a spacing of 0.1 m to measure the pressure induced by the sloshing of the liquid. Three pressure transducers (P6-P8) were housed on the top panel to measure the impact due to sloshing of the liquid. The scaled tank details are shown in Fig. 3. The linear approximation of the nth mode liquid sloshing frequency, f_n by Ibrahim (2005) is given as

$$f_n = \frac{1}{2\pi}\sqrt{\frac{n\pi g}{l}\tanh\left(\frac{n\pi h_s}{l}\right)} \quad n=1, 2, 3\ldots\ldots \tag{1}$$

where, l is the length of the tank h_s is the static liquid depth and n is the surface mode number.

The sloshing modal frequencies to second decimal accuracy for the different fill depths (h_s) are provided in Table 1. Porous baffle walls with porosities of 15%, 20.2% and 25.2% are prepared by using acrylic sheet of thickness 5 mm and are shown in Fig. 4. A pore size of diameter 15 mm was adopted for all the porosities

considered. The centre to centre distances are 45 *mm*, 36 *mm* and 31 *mm* for the porosities of 15%, 20.2% and 25.2%, respectively and the staggered arrangement of pores on the baffle wall is shown in Fig. 5. The different baffled tank configurations adopted in the present study is depicted in Fig. 6.

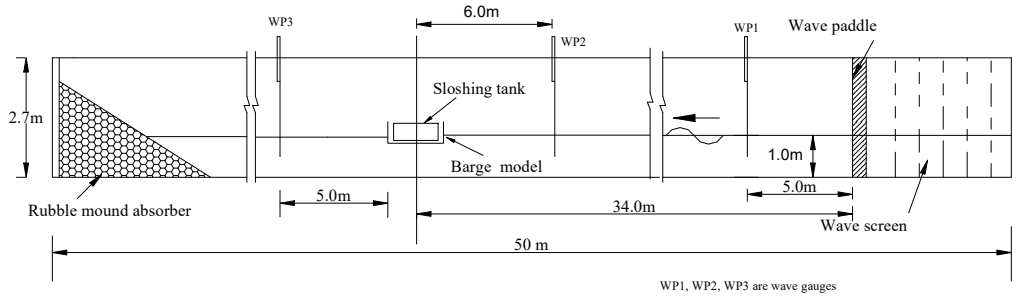

Fig. 2: Experimental setup in the wave flume

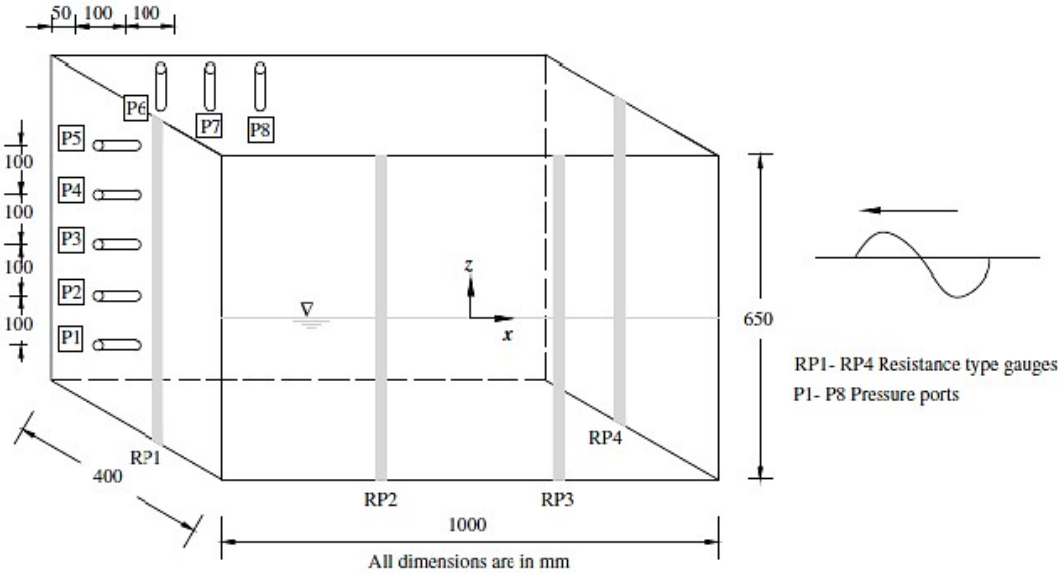

Fig. 3: Schematic sketch of sloshing tank model details

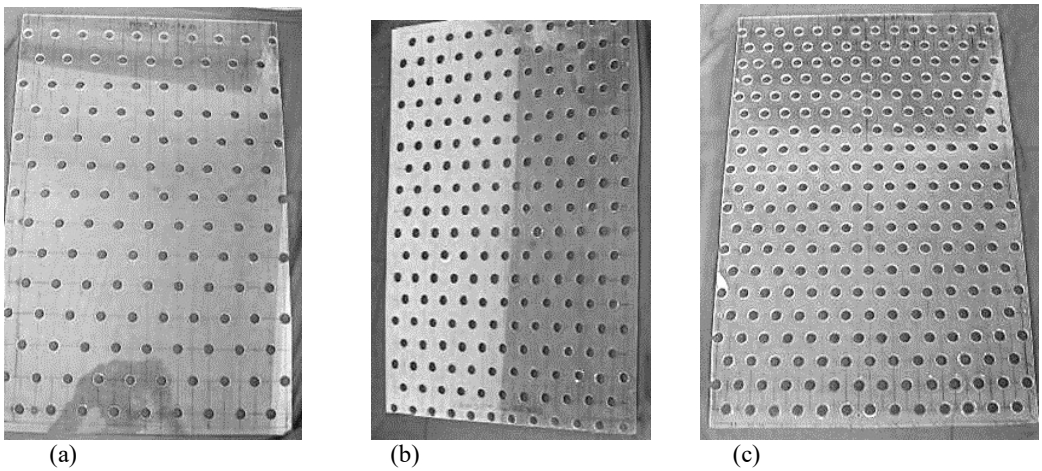

(a) (b) (c)

Fig. 4: Porous baffles (a) 15%, (b) (20.2% and (c) 25.2%.

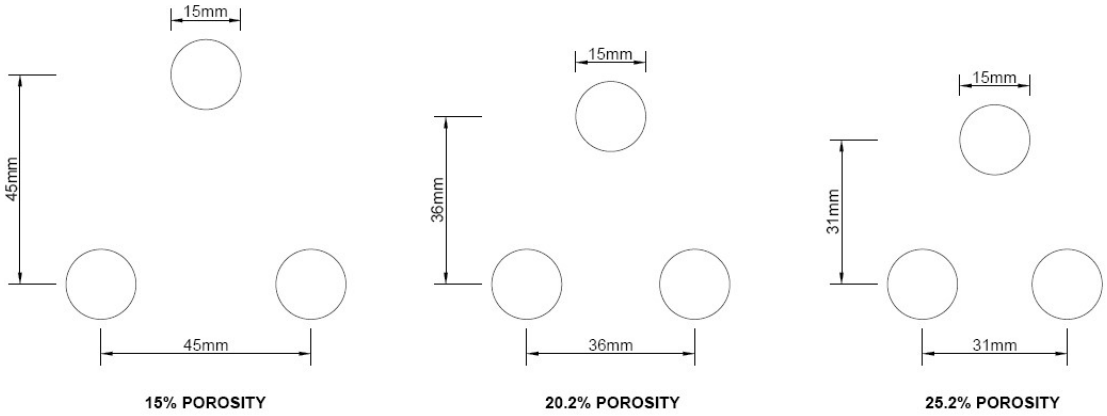

Fig. 5: Staggered arrangement of pores in a baffle.

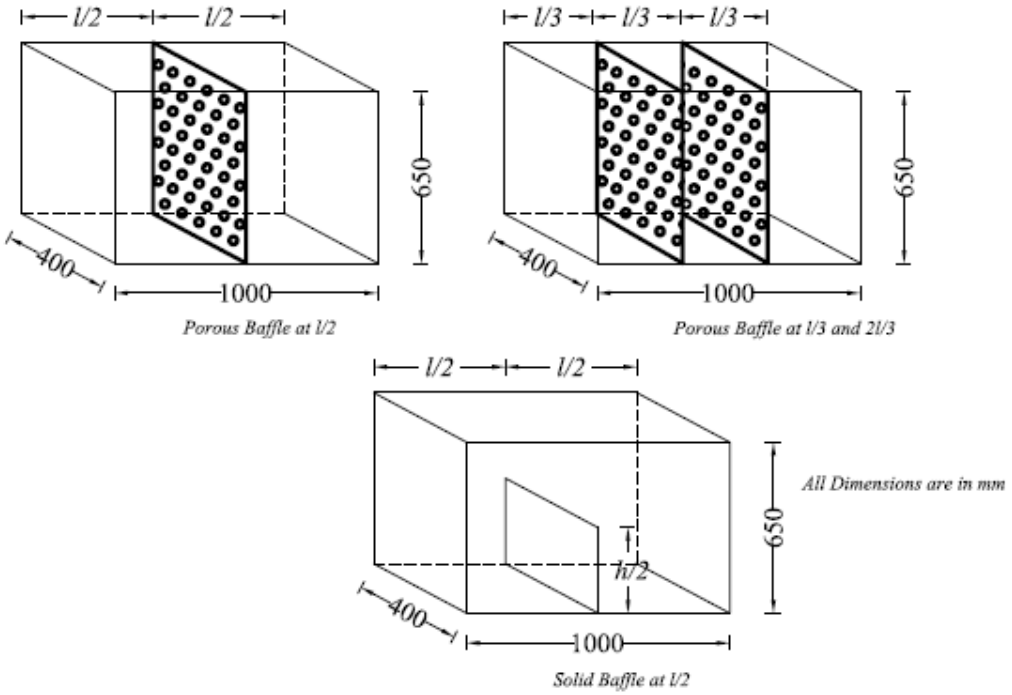

Fig. 6: Baffle arrangements inside a sloshing tank.

Faltinsen and Timokha (2009) proposed the modified equations of sloshing frequencies for centrally placed bottom mounted and surface flushing vertical baffle in a 2-D sloshing tank are given in Eqn. (2) and Eqn. (3), respectively. In order to understand the effect of baffles on dissipating sloshing energy and consequent reduction in sloshing pressure, the modified sloshing frequencies for the baffled tank is also provided in Table 1.

$$\frac{\omega_1'^2}{\omega_1^2} = 1 - \frac{2\pi^2 \sin^2(\pi/2)}{\sinh(2\pi h_s/l)}\left(\frac{h_b}{l}\right)^2 \tag{2}$$

$$\frac{\omega_1'^2}{\omega_1^2} = 1 - \frac{\pi^2 \sin^2(\pi/2)}{\tanh(\pi h_s / l)} \left(\frac{h_b}{l}\right)^2 \quad (3)$$

where, h_b is height of baffle

The model parameters of the barge with 75% liquid filled in the sloshing tank is given in Table 2. An equivalent dry weight condition is considered for the comparison purpose and the barge natural frequencies in heave and roll modes are deduced from the free decaying response of the barge in calm water. The barge frequencies are compared with predicted values and are listed in Table 2. An incident regular wave height of 0.1 *m* was adopted for the present experimental program. The wave excitation frequency (f_w) was varied between 0.46 and 1.54 *Hz* and the wave climate details are given in Table 3. The signals from the resistive gauges, the pressure transducers and accelerometers were continuously acquired for time duration of 60-90 *s* with sampling frequency of 40 *Hz* and collected through a DHI wave amplifier, a d.c. amplifier, and a carrier frequency amplifier, respectively. The data collection is directly controlled by 12 bit resolution A/D card.

Table 1: Tank sloshing frequencies for 75% fill depth

	$f_1(Hz)$	$f_2(Hz)$	$f_3(Hz)$	$f_4(Hz)$	$f_5(Hz)$
Without Baffle (Eqn.1)					
Tank length, l	0.84	1.25	1.53	1.77	1.98
f_n/f_1, n = 1, 2, 3,……	1	1.48	1.82	2.09	2.34
Tank length, $l/2$	1.25	1.77	2.16	2.50	2.79
f_n/f_1, n = 1, 2, 3,……	1.0	1.42	1.74	2.0	2.23
Tank length, $l/3$	1.53	2.16	2.65	3.06	3.42
f_n/f_1, n = 1, 2, 3,……	1.0	1.41	1.73	2.0	2.24
Submerge Solid Baffle @ $l/2$ (Eqn.2) ($h_b = h/2$)	0.75	1.12	1.38	1.59	1.77
f_n/f_1, n = 1, 2, 3,……	1	1.49	1.84	2.12	2.36

Table 2: Barge model parameters and barge frequencies

Fill depth in sloshing tank $h_s = (h^*\ \%)$	Draft of barge (m)	Total mass (kg)	KG (m)	$(MI)_{CG}$ ($kg\text{-}m^2$)
0.75	0.123	293	0.260	54.83
Draft of barge (m)	Experimental Analysis (f_z)	Eigen value Analysis (FEM) (f_z)	Experimental Analysis (f_ϕ)	Eigen value Analysis (FEM) (f_ϕ)
0.123	0.67	0.66	0.81	0.81

Table 3: Adopted wave parameters

Test Case	Fill depth $h_s = (h^*\ \%)$	Incident wave height, H_i (m)	Wave frequency range, $f_w(Hz)$
Without baffle	0.75	0.1	0.46 – 1.54
With baffle [Submerged solid baffle and Porous baffle (15%, 20.2% and 25.2% porosities)]	0.75	0.1	0.46 – 1.54

3. Results and Discussions

3.1 Barge responses

The steady state barge responses, sway (X), heave (Z) and roll (ϕ) is considered to analyse the characteristics of barge RAOs'. The partially liquid filled condition, partially liquid filled with different placement of baffled conditions and equivalent dry weight conditions are compared. The RAOs' for dry weight condition is obtained by solving linear radiation and diffraction problem using the Finite Element Method (FEM) procedure of Sannasiraj *et al.* (1995) The characteristics of barge Response Amplitude Operators (RAO) for 75% liquid filled condition and the corresponding equivalent dry weigh conditions are detailed in Nasar *et al.* (2010). The influence of the placement of baffled conditions on RAOs' is reported in Fig. 7, Fig. 8 and Fig. 9 for porosities of 15%, 20.2% and 25.2%, respectively. A detailed investigation reveals that an inconsequence of porous baffles is noted on the characteristics of heave and roll RAOs', however, the peak amplitude of roll RAO is further reduced. It is observed that the sway RAO is influenced by the presence of porous baffles between the excitation ratio (f_w/f_1) of 0.6 and 1.2 wherein sloshing oscillation is high and in turn affect the sway response. Also, increase in sway response might be due to the synchronizing of phase between sway oscillation and sloshing flow. However, sloshing is a resonance phenomena, higher sway amplitude at certain frequencies is not helpful in increasing the sloshing run-up.

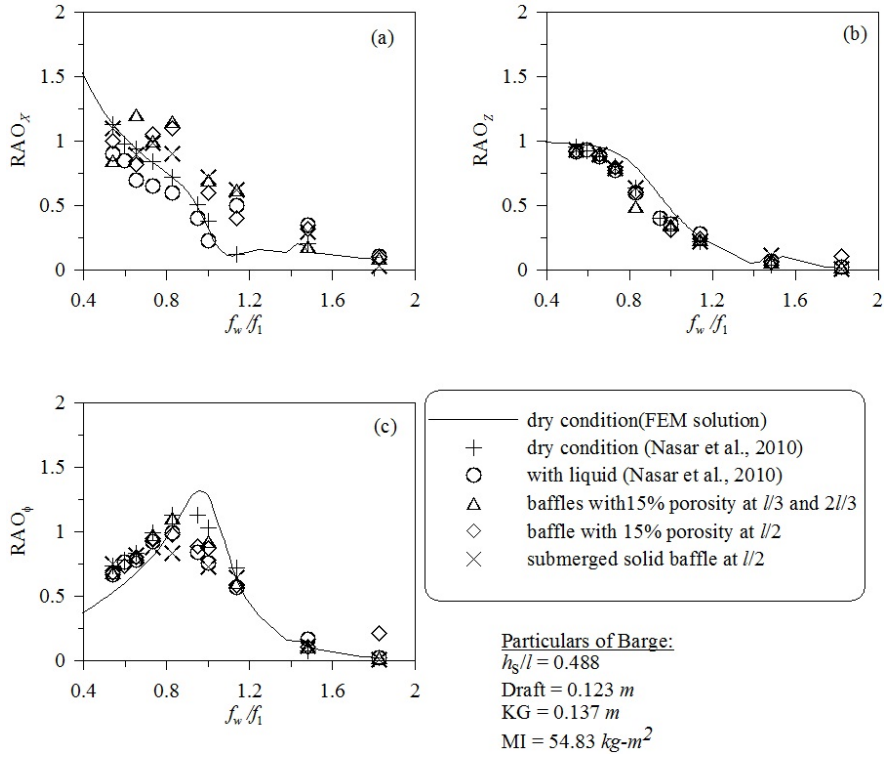

Fig. 7: Response amplitude operator of the barge for the draft of 0.123 m and 15% porosity baffles: (a) sway (b) heave and, (c) roll

3.2 Analysis of sloshing pressure

3.2.1 General

The liquid-sloshing behaviour in the partially filled tank depends on the excitation frequency and amplitude, size of the tank, geometry of the tank (rectangular, square and cylindrical), liquid-filled depth and internal baffle arrangements, if any. Consequently, the sloshing pressure may be of non- impulsive (due to formation of standing wave) or impulsive type (Akyildiz and Unal, 2005). Various authors reported the possibility of different types of wave formation at different water depths and the resulting sloshing pressure.

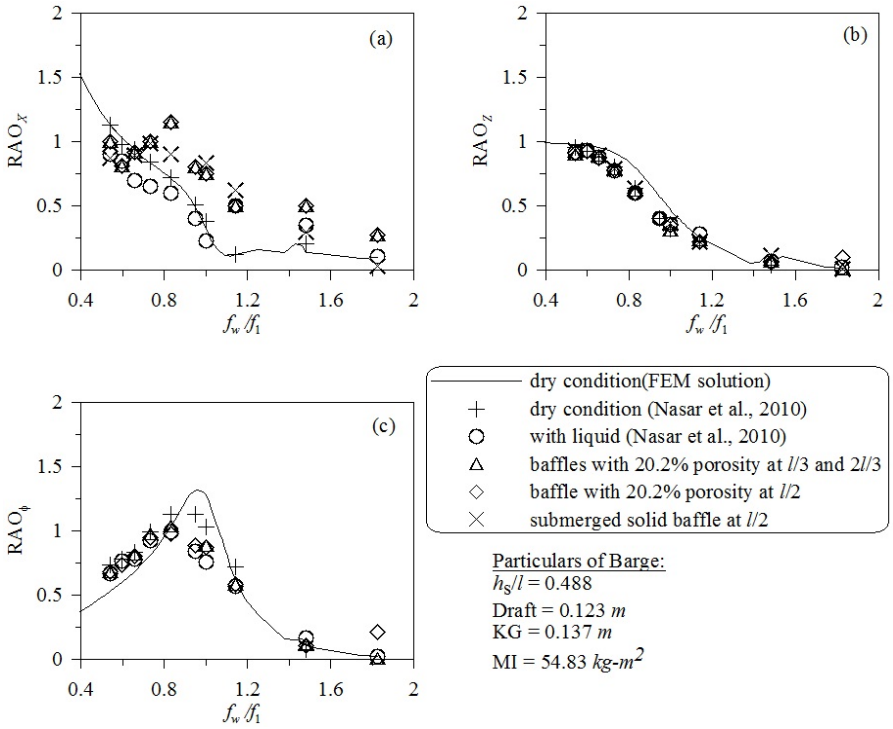

Fig. 8: Response amplitude operator of the barge for the draft of 0.123 m and 20.2% porosity baffles: (a) sway (b) heave and, (c) roll

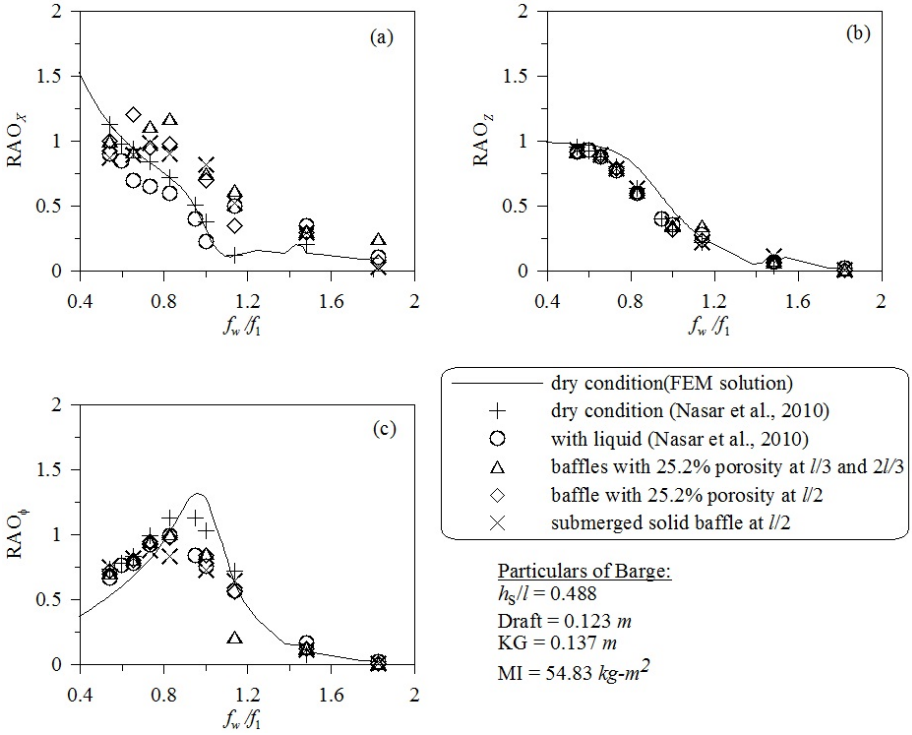

Fig. 9: Response amplitude operator of the barge for the draft of 0.123 m and 25.2% porosity baffles: (a) sway (b) heave and, (c) roll

Faltinsen and Timokha (2001) reported the standing wave formation in finite water depth. Kim *et al.* (2007) observed the formation of progressive wave resulted an impact load on the side wall panels of a tank with abrupt change in tank geometry at high filling levels. Ockendon *et al.* (1986) enunciated the formation of travelling wave, bore phenomena, high run up on tank walls and hydraulic jump at shallow liquid fill level. Kim (2001) examined the types of wave formation and the resulting sloshing pressure in a partially filled tank equipped with side stringers and a bottom mounted vertical baffle which are a typical LNG tank configuration. The liquid tank system was subjected to sway/surge, pitch/roll, combined sway/surge (with and without phase difference), and combined pitch/roll (with and without phase difference) mode of excitation. The following salient results are drawn. At shallow filling levels, the side stringers experience high slamming load. At higher filling levels, the internal members are less effective in reducing occurrence of impact on tank ceilings and on corners. The sloshing flow was observed to be rapid above the location of vertical member and results in high impact on tank wall. In the present work, the effectiveness of baffles (bottom mounted vertical porous baffle and submerged solid baffle) at 75% filling level with an aspect ratio of 0.488 is discussed. Typical time histories of sloshing oscillations and pressure (p) at various levels of the tank subjected to regular wave excitation frequency of 0.96 Hz for without baffle wall condition and with porous baffle of porosity 15% is shown in Fig. 10.

3.2.2 Without baffle wall condition

The variation of dimensionless root mean square (*rms*) pressure (p_c^{rms}/H_i) measured at pressure port location, P4 with excitation frequency ratio (f_w/f_1) ranging from 0.54 to 1.83 and for two different relative incident wave heights (H_i/d=0.08 and H_i/d=0.1) is shown in Fig. 11. It can be seen that the effect of wave height is minimal, however, effect of frequency is prominent and hence sloshing is frequency dependent phenomenon. For H_i/d=0.1, p_c^{rms}/H_i is found to be maximum at excitation frequency ratio f_w/f_1=1.14 which corresponds to f_w=0.96 *Hz* and the maximum is about 1.2 times the pressure response observed at f_w/f_1=1. As a result of violent sloshing at f_w=0.96 *Hz*, an impact of liquid is observed on the top panel and time traces observed by pressure ports (P7 and P8) are shown in Fig. 12. The maximum impact (p^c_{max}/H_i) and rms pressure (p^c_{rms}/H_i) within the time history are presented in Fig. 13. The impact pressures, p^c_{max}/H_i and p^c_{rms}/H_i at the ceiling of sloshing tank and at pressure port location P7 is about 2.2 times and 1.5 times of the pressure observed at pressure port location P4. The above said variations at P8 are learnt to be about 125% and 90% of the pressure observed at P4.

3.2.3 Porous baffle at l/2

Porous baffle walls considerably suppress the sloshing motion and it is expected that there would be significant reduction in sloshing pressure on the liquid containment. The pressure fluctuations at pressure port locations near to the free surface is pragmatic to be high compared to deeper surface in the liquid sloshing tank (Panigrahy *et al*., 2009). Hence, the discussion is presented for pressure port location (P4) by considering the fact that the free surface exists just above the P4. Porous baffle of porosities 15%, 20.2% and 25.2% placed at centre of the tank are studied in detail. The effectiveness of porous baffles or reduction in sloshing pressure in a baffled tank is calculated as follows:

$$Percentage\ of\ attenuation\ =\ \frac{\left[\zeta_{\max}(without\ baffle)-\zeta_{\max}(with\ baffle)\right]}{\zeta_{\max}(without\ baffle)}\text{x}100 \tag{4}$$

The resulting sloshing pressure time traces due to steady state oscillation is considered for the analysis. Within the time history, the crest values are picked up and the root mean square of sloshing pressure (p^c_{rms}/H_i) and maximum sloshing pressure (p^c_{max}/H_i) are obtained. The variation of p^c_{rms}/Hi with f_w/f_1 at vertical wall (z/h_s) for without baffle condition, porous baffles placed at *l*/2 for three different porosities of 15%, 20.2% and 25.2% are shown in Fig. 14, Fig. 15, Fig. 16 and Fig. 17, respectively. It is realised that there are fluctuations in sloshing pressure at pressure port location P4 (z/h_s=-0.18) for all the excitation frequencies (f_w/f_1=0.54-1.83) considered. Also it is noticed that the dynamic pressure decrease as the depth increases. The maximum variation is observed at all pressure port locations for a wave excitation frequency of 0.96 *Hz* (f_w/f_1=1.14) among the excitation frequencies considered. For without baffle condition and by considering the *rms* crest pressure at P4 (Fig. 14)**,** the non-dimensional pressure decreases from 0.49 to 0.02 over frequency ratio (f_w/f_1) of 1.14 to 1.83. Further, the pressure decreases from 0.43 to 0.07 as the frequency ratio varies between 1.0 and 0.54. In similar manner, the said variation due to baffle wall with 15% porosity (Fig. 15) is from 0.24 to 0.18 and 0.23 to 0.05 over the frequency ratio (f_w/f_1) of 1.14 to 1.83 and 1.0 to 0.54, respectively. The same trend of variation is noticed for the baffle wall with 20.2% (Fig. 16) and 25.2% (Fig. 17) porous conditions as well.

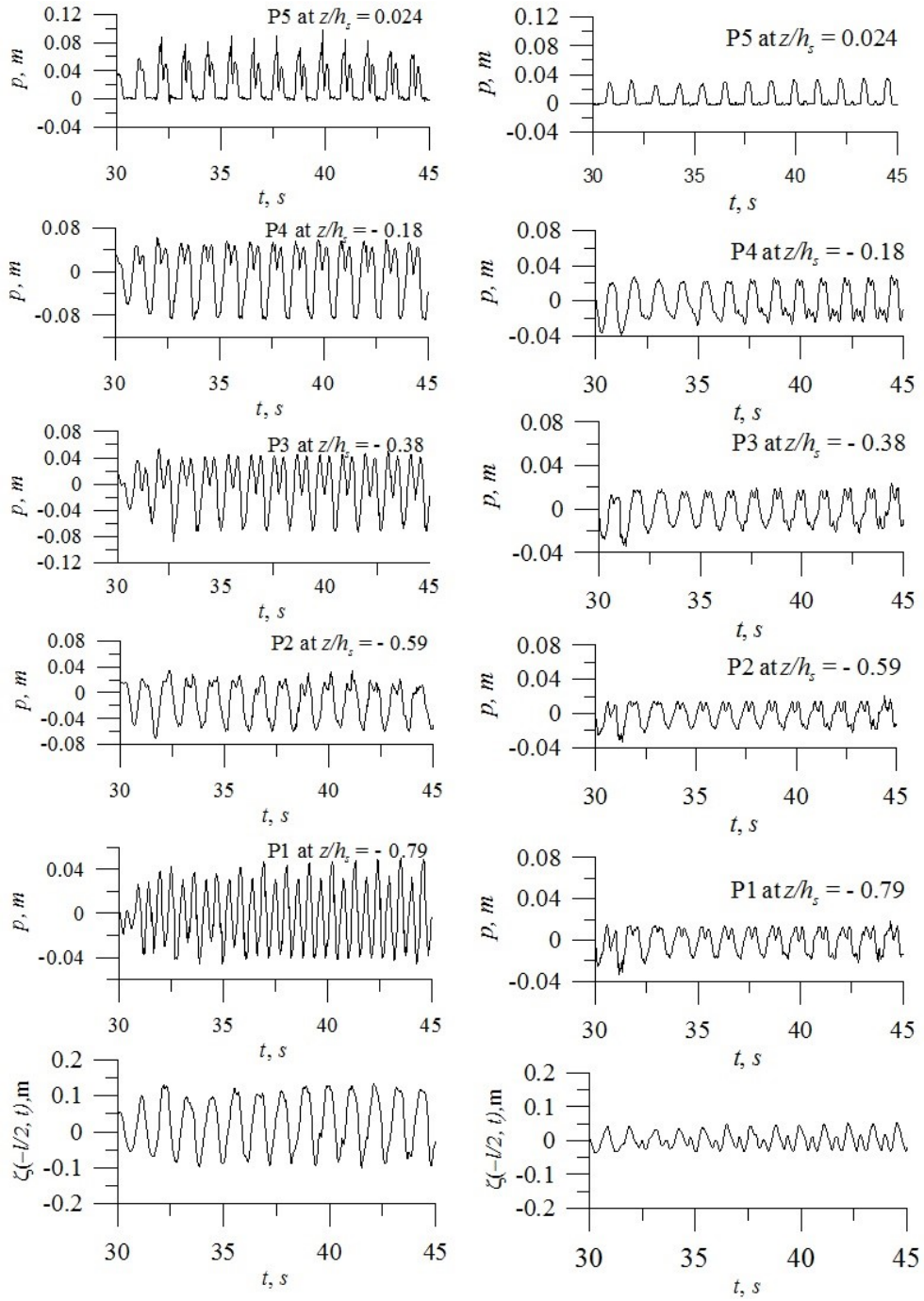

Fig. 10: Sloshing motion (ζ) and pressure (p) on the tank walls for h_s/l=0.488 and f_w=0.96 *Hz* for (a) Without baffle condition and (b) Baffle of porosity 15%

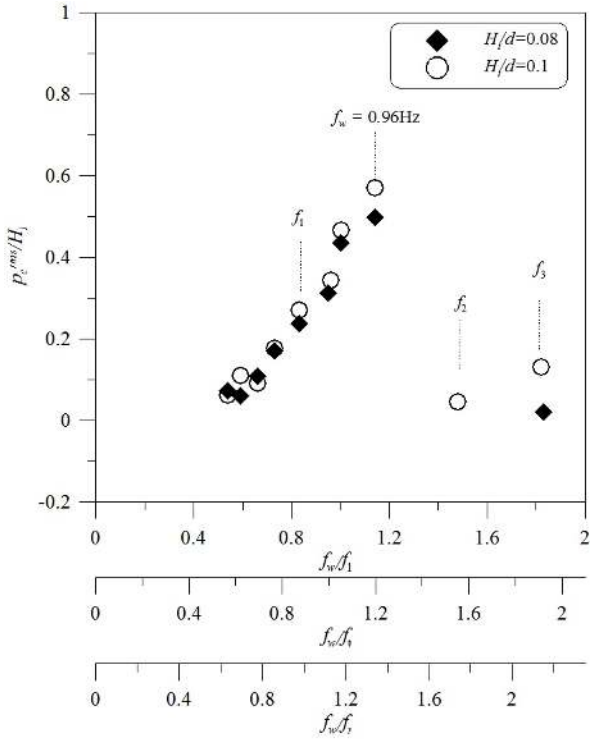

Fig. 11: Variation of p^c_{rms} / H_i with f_w/f_1 at P4(z/h_s=-0.18) for H_i/d=0.10 and h_s/l=0.488

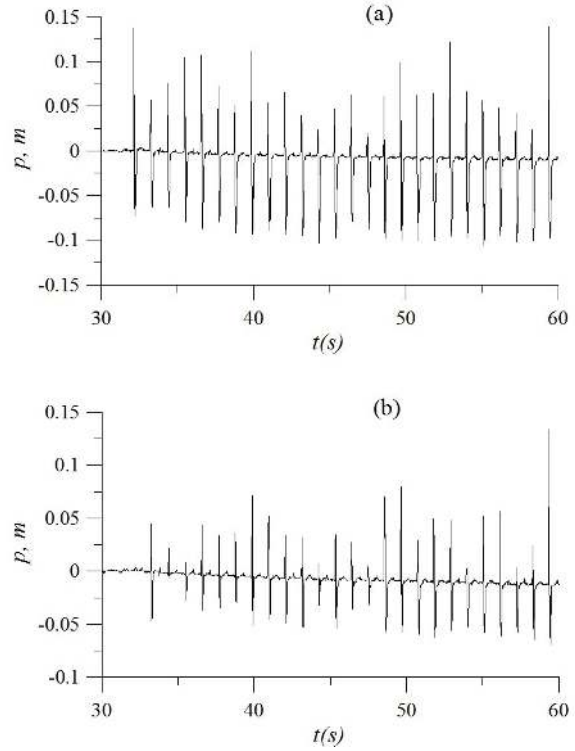

Fig. 12: Impact pressure on tank ceiling on various locations for f_w =0.96 *Hz*, H_i/d =0.10 and h_s/l =0.488: (a) P7(x/l = -0.35) and (b) P8(x/l = -0.25)

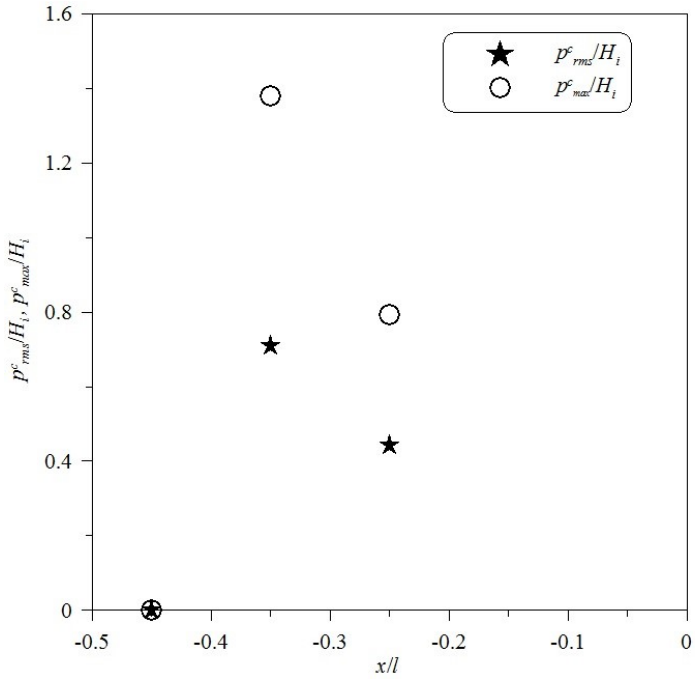

Fig. 13: Variation of p^c_{rms}/H_i and p^c_{max}/H_i on tank ceiling (x/l) with H_i/d= 0.10 and h_s/l =0.488

The variation of p^c_{rms}/H_i and p^c_{max}/H_i with f_w/f_1 at pressure port location P4 for all the porosities and also the percentage reduction in pressure are shown in Fig. 18 and Fig. 19, respectively. For without baffle wall and the baffle wall with all the porosities considered, the maximum responses of p^c_{rms}(Fig. 18a) and p^c_{max}/H_i (Fig. 19a) are observed at excitation frequency of 0.96 *Hz* (f_w/f_1=1.14). The variation in percentage of reduction of sloshing pressure in comparison with without baffle condition (Equ.4) is calculated (Fig. 18b & Fig. 19b) and the discussion is as follows. The percentage reduction in p^c_{rms} for 15% porosity is about 51% at f_w/f_1=1.14. The said value of reduction for p^c_{max} is about 65%. However, the reduction in sloshing pressure (p^c_{rms}) at f_w/f_1=1 is about 48% whilst p^c_{max} is reduced by 42%. For other than natural sloshing frequencies (out of resonance frequencies) i.e., for f_w/f_1=0.83,0.73,0.66 and 0.54, the reduction in sloshing pressure (p^c_{rms}) is about 27%, 28%, 19% and 31%, respectively. In similar manner, the above said reduction in p^c_{max} is about 12%, 27%, 16% and 18% for excitation frequency ratios of 0.83, 0.73, 0.66 and 0.54, respectively. Baffle with 15% porous condition gives an undesirable response in reducing the sloshing pressure at wave excitation $f_w = f_3$ *Hz* and the reductions in p^c_{rms} and p^c_{max} are about -678% and -360%, respectively.

As observed for 15% porous condition, 20.2% porosity exhibits maximum reduction in rms sloshing pressure (p^c_{rms}) and in p^c_{max} at wave excitation frequency (f_w) of 0.96 *Hz* and are about 54% and 68%, respectively. Whilst f_w is equal to first mode sloshing frequency i.e., $f_w = f_1$ *Hz* (f_w/f_1=1.0), the dissipation in sloshing pressure is about 48% and for the same frequency ratio, the p^c_{max} reduces by 36%. As the wave excitation frequency ratio (f_w/f_1) varies from 0.95 to 0.54, the dissipations in p^c_{rms} are about 27%, 18%, 34%, 18%, 21% and 26% for ratio of (f_w/f_1) 0.95, 0.83, 0.73, 0.66, 0.59 and 0.54, respectively and reduction in p^c_{max} are 36%, 46%, 22%, 12%, 29% 30% and 24%, respectively. With increase in porosity from 20.2% to 25.2%, the dissipations in pressure of p^c_{rms} and p^c_{max} are found to be about 51% and 62%, respectively at wave excitation of 0.96 *Hz*. For the excitation at resonance frequencies f_1 and f_3, 25.2% porous wall dampening the sloshing pressure, p^c_{rms} by 43% and -388%, respectively. The said dampening in p^c_{max} are about 40% and -192% at $f_w = f_1$ and $f_w = f_3$, respectively. As the wave frequency ratio varies from (f_w/f_1) 0.83 to 0.54, the reduction in p^c_{rms} are about 27%, 16%, 11%, 10%, and 48% for ratio of (f_w/f_1) 0.83, 0.73, 0.66 and 0.54, respectively and reductions in p^c_{max} are 18%, 14%, 19% and 17%, respectively. It can be noticed that all the porous conditions are ineffective in dissipating the sloshing energy and resulting sloshing pressure at $f_w=f_3$. Herein, the excitation ratio of 1.82 ($f_w=f_3$) satisfies primary resonance of third mode (f_w/f_1=1.84) in submerged solid baffle condition (Refer Table 1) and increases the participation of third mode compared with unbaffled condition.

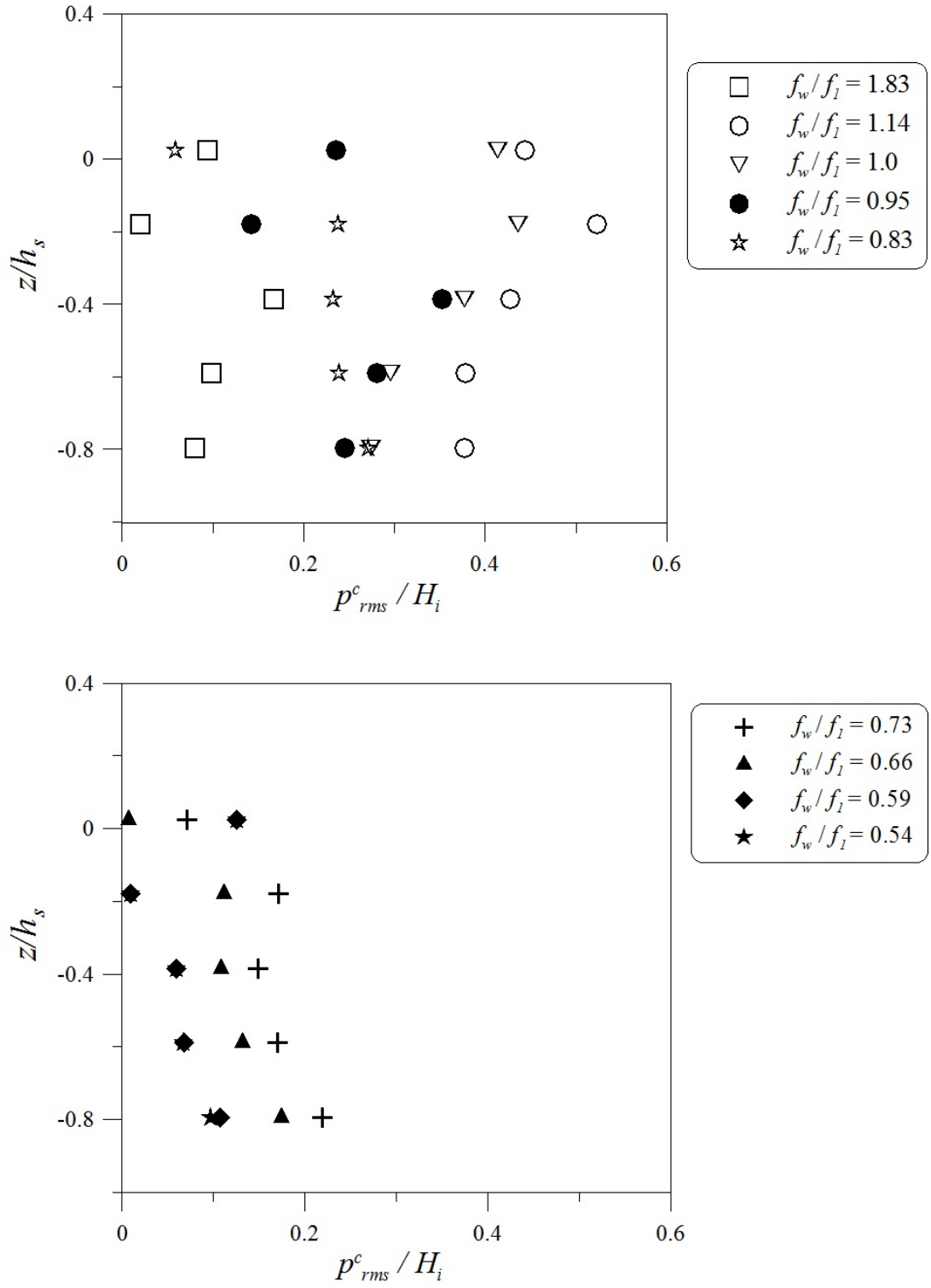

Fig. 14: Variation of p_c^{rms}/H_i at vertical wall (z/h_s) with f_w/f_1 for H_i/d=0.10 and h_s/l=0.488 (without baffle)

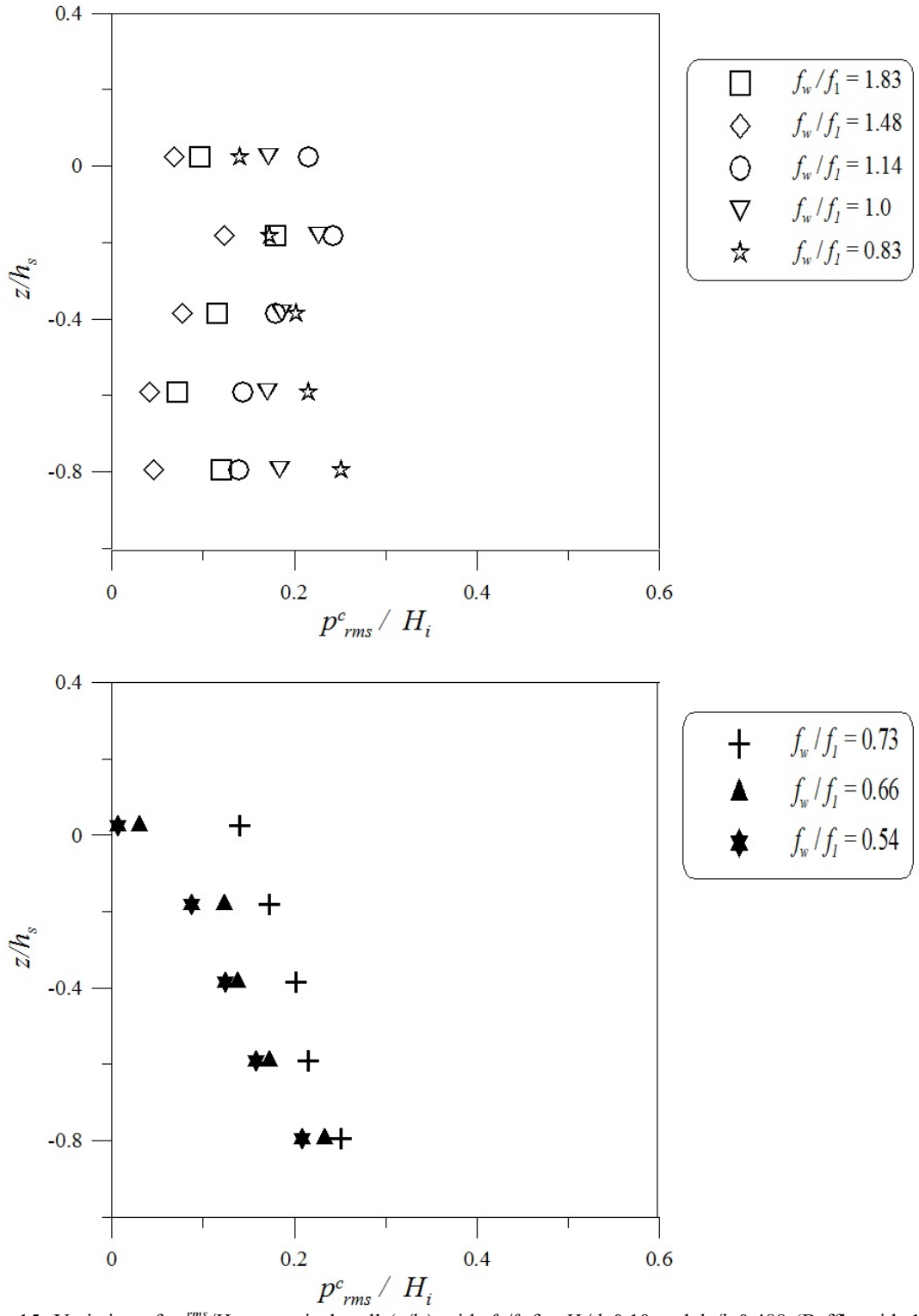

Fig. 15: Variation of p_c^{rms}/H_i at vertical wall (z/h_s) with f_w/f_1 for H_i/d=0.10 and h_s/l=0.488 (Baffle with 15% porous condition and placed at $l/2$)

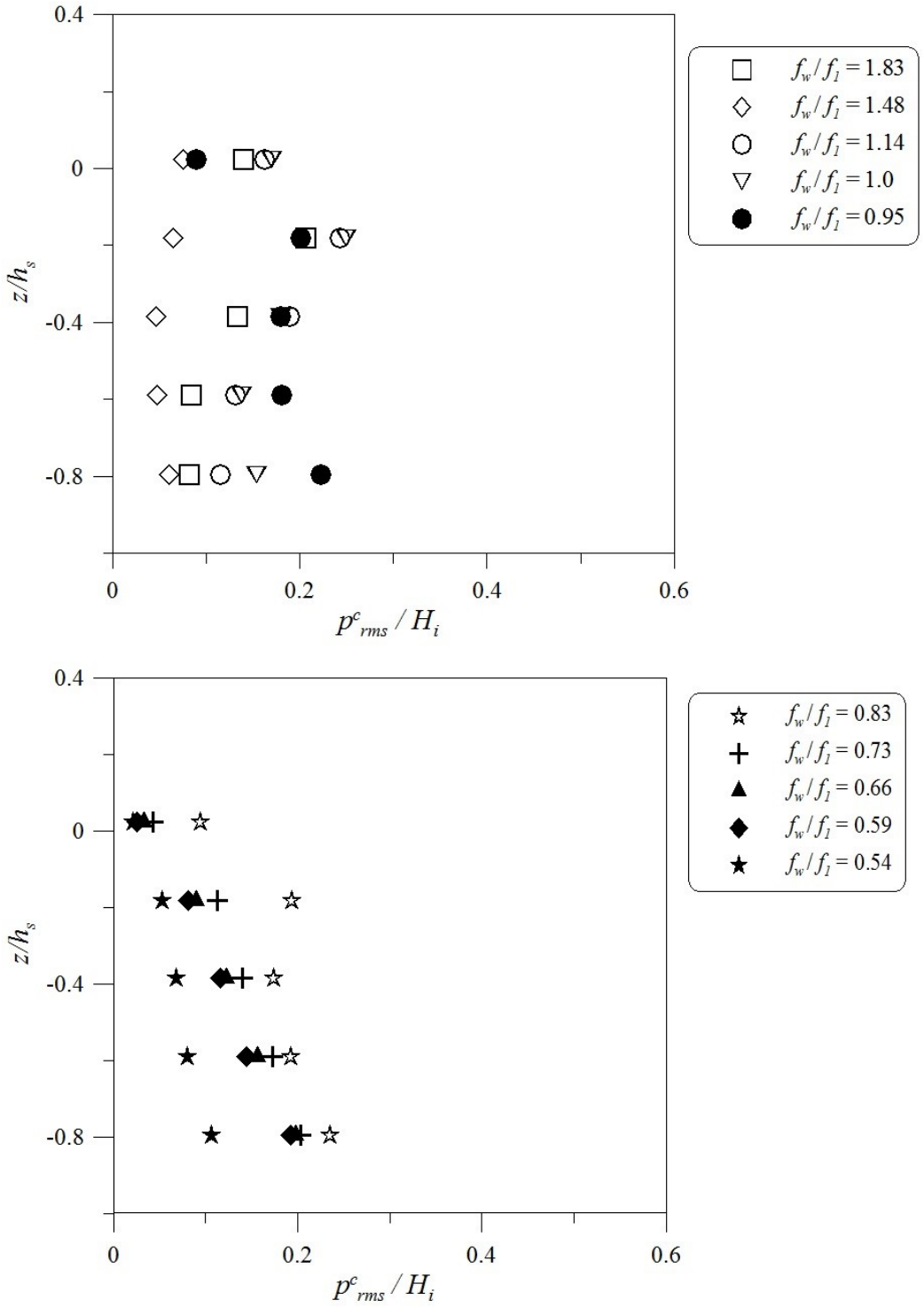

Fig. 16: Variation of p_c^{rms}/H_i at vertical wall (z/h_s) with f_w/f_1 for H_i/d=0.10 and h_s/l=0.488 (Baffle with 20.2% porous condition and placed at $l/2$)

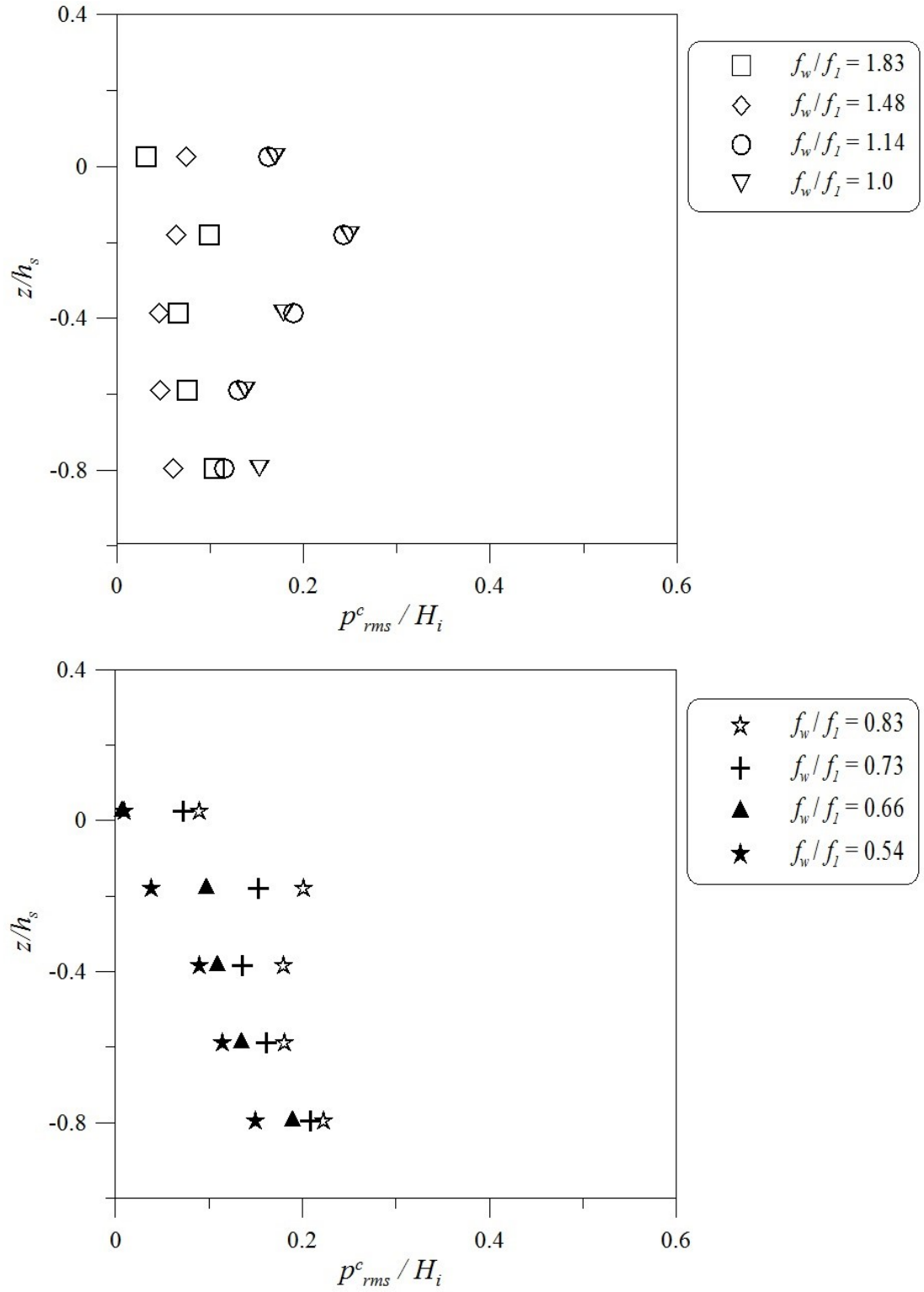

Fig. 17: Variation of p_c^{rms}/H_i at vertical wall (z/h_s) with f_w/f_1 for H_i/d=0.10 and h_s/l=0.488 (Baffle with 25.2% porous condition and placed at $l/2$)

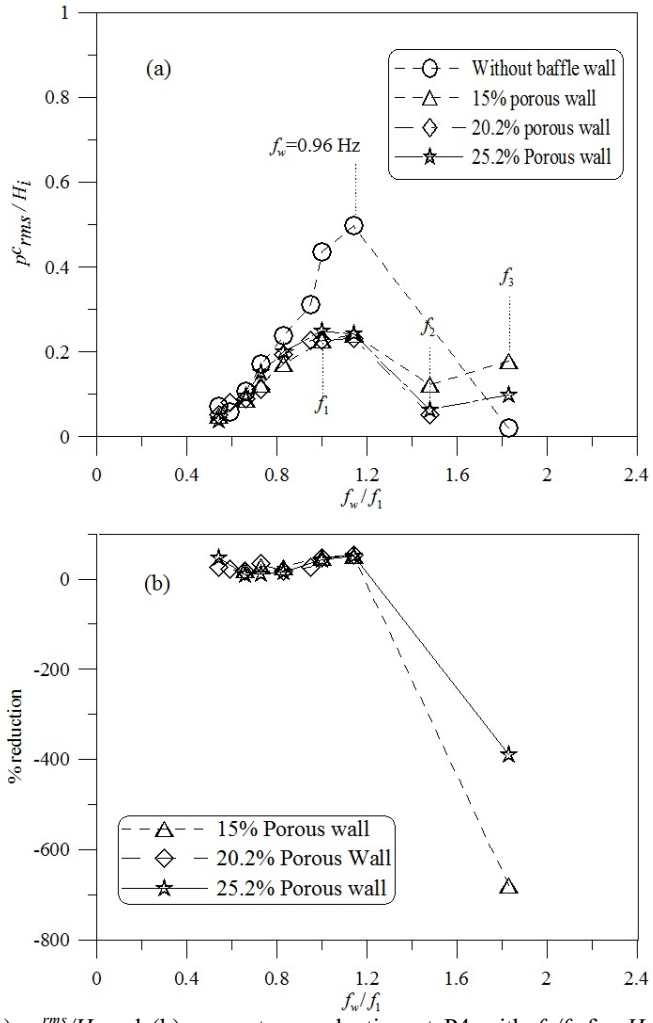

Fig. 18: Variation of (a) p_c^{rms}/H_i and (b) percentage reduction at P4 with f_w/f_1 for H_i/d=0.10 and h_s/l=0.488 (Baffle placed at *l/2*)

3.2.4 Porous baffles at l/3 and 2l/3

In order to understand the effect of placement in reducing the sloshing pressure, the porous walls placed at *l/3* and *2l/3* of the sloshing tank length, *l* is considered. The same wave climate is adopted as used for baffle wall placed at *l/2* and the test setup was subjected to excitation frequency range of 0.45 *Hz* to 1.54 *Hz*. The variation of p^c_{rms}/H_i with different frequency ratio (f_w/f_1) at vertical wall (z/h_s) for three different porosities of 15%, 20.2% and 25.2% are shown in Fig. 20, Fig. 21 and Fig. 22, respectively. As experienced by porous baffle placed at *l/2*, a high fluctuation is noticed at pressure port location, P4 for all the excitation frequencies considered and the variation of pressure at P4 location is taken into consideration for further analysis. The baffle with 25.2% porosity provides maximum non dimensional (p^c_{rms}/H_i) response of 0.13 at frequency ratio (f_w/f_1) of 1.14, however, a maximum response of 0.17 is obtained at frequency ratio of 1.0 for both 15% and 20.2% porosities. A decrease in trend is observed in *rms* crest pressure (p^c_{rms}/H_i) as the frequency ratio varies from 0.95 to 0.54 for all the porosities considered. For wave excitation at frequency ratio of 1.83 (which corresponds to third mode frequency), the non-dimensional *rms* crest pressure at port P4 are 0.08, 0.13 and 0.21 for 15%, 20.2% and 25.2% porosities, respectively.

The variation of dimensionless pressures, p^c_{rms}/Hi and p^c_{max}/Hi with f_w/f_1 measured at pressure port location, P4 are shown in Fig. 23a and Fig. 24a, respectively and the corresponding percentage reduction in sloshing pressure for all the porosities are shown in Fig. 23b and Fig. 24b, respectively. For without baffle wall condition, the maximum responses of p^c_{rms} (Fig. 23a) and p^c_{max}/Hi (Fig. 24a) are observed at excitation frequency of 0.96 *Hz*

(f_w /f_1=1.14). At f_w = f_3, pressure responses are amplified for all the porosities considered, in which, 25.2% porous condition showing highest inferior performance. The porous wall with 15% porosity reduces the pressures p^c_{rms} (Fig. 23b) and p^c_{max} (Fig. 24b) by 75% at excitation frequency ratio (f_w/f_1) of 1.14. The dissipation in pressure responses (p^c_{rms} and p^c_{max}) observed at f_w /f_1=1 is tendered by an average amount of 60%. At out of resonance frequencies ratio, f_w /f_1=0.83,0.73,0.66 and 0.54, the dissipation in p^c_{rms} is about 51%, 48%, 29% and 53%, respectively. In similar manner, the above said reduction in p^c_{max} is about an average of 45% for excitation frequency ratio varies from 0.83 to 0.54. However, it is noticed that the porous baffle doesn't serve the purpose at wave excitation frequency f_w= f_3 *Hz* (Fig. 23b and Fig. 24b) and the pressures p^c_{rms} and p^c_{max} are increased by 3 and 1.5 times, respectively on comparison with unbaffled condition.

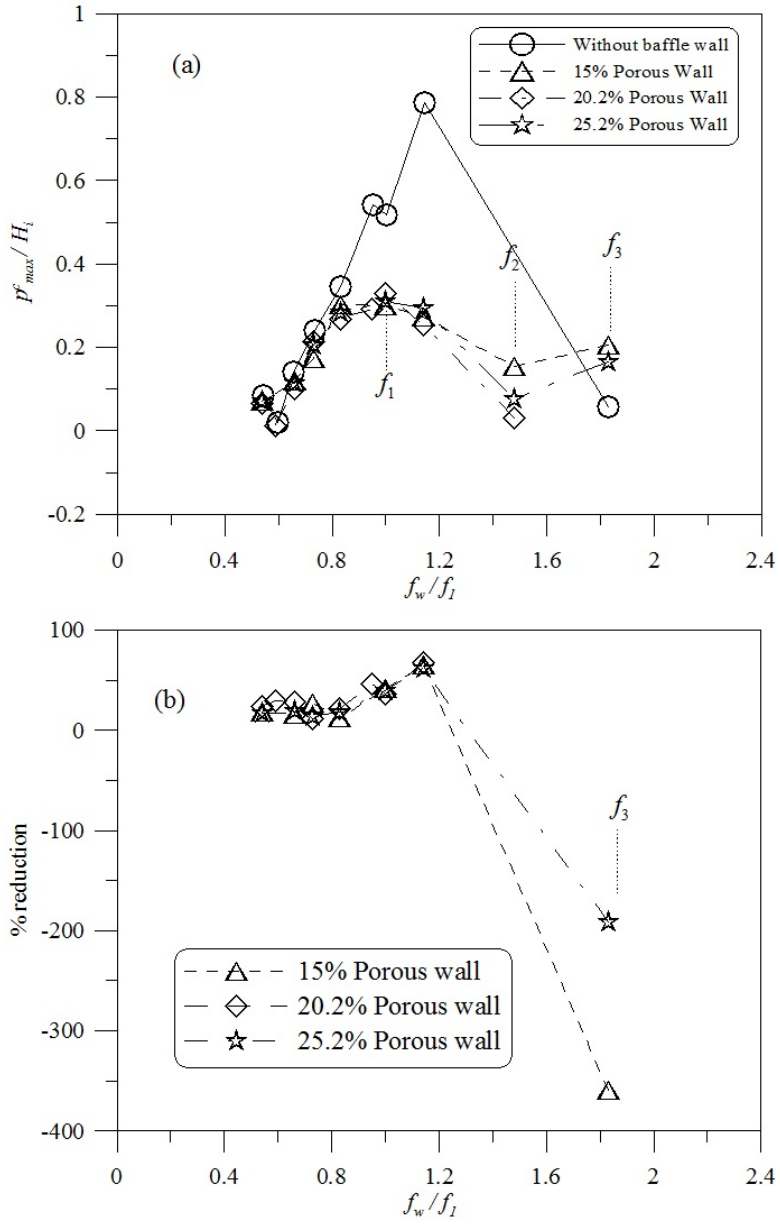

Fig. 19: Variation of (a) p^c_{max}/H_i and (b) percentage reduction at P4 with f_w/f_1 for H_i/d=0.10 and h_s/l=0.488 (Baffle placed at *l/2*)

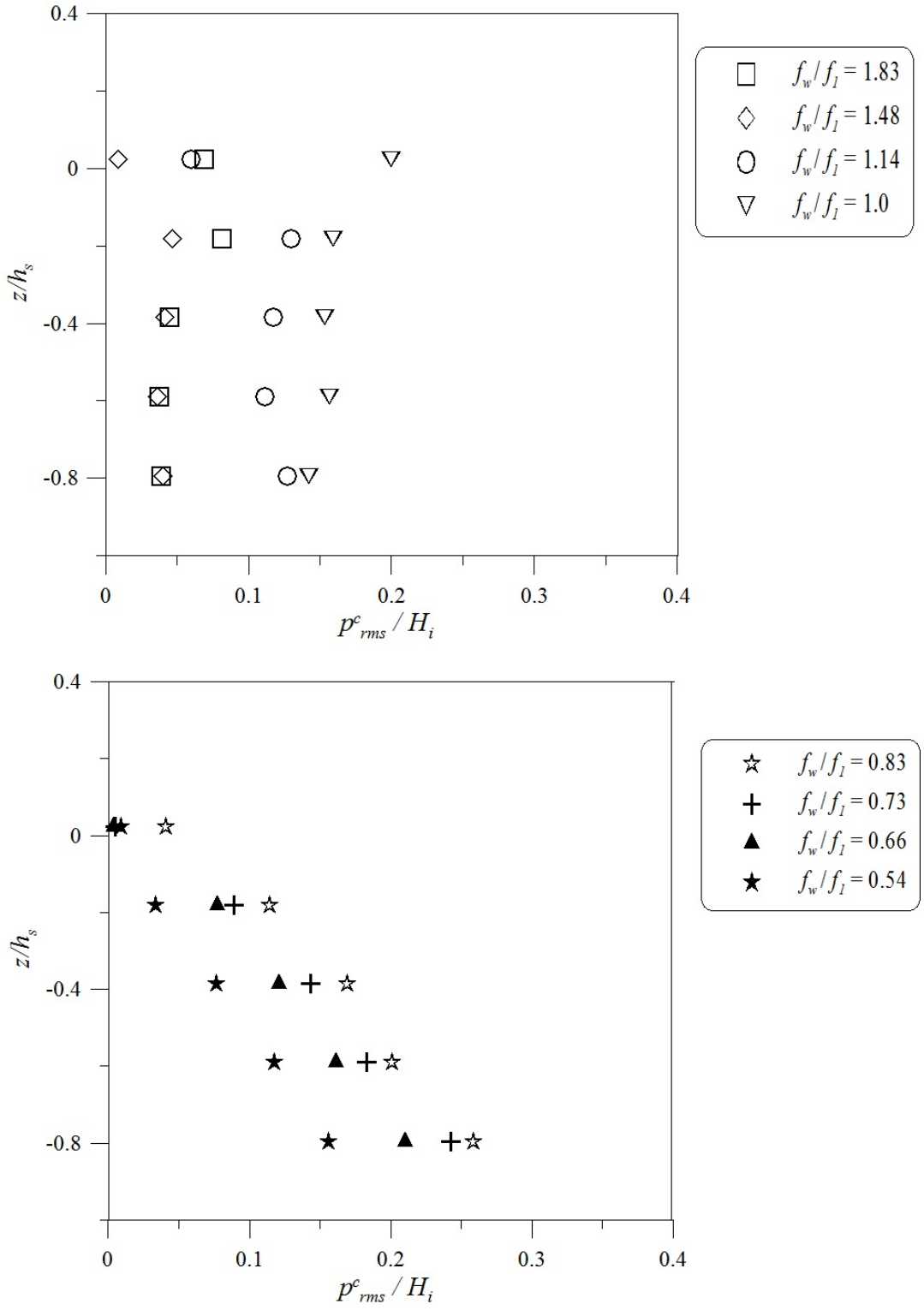

Fig. 20: Variation of p_c^{rms}/H_i at vertical wall (z/h_s) with f_w/f_1 for H_i/d=0.10 and h_s/l=0.488 (Baffle of porosity =15% and placed at *l/3* and *2l/3*)

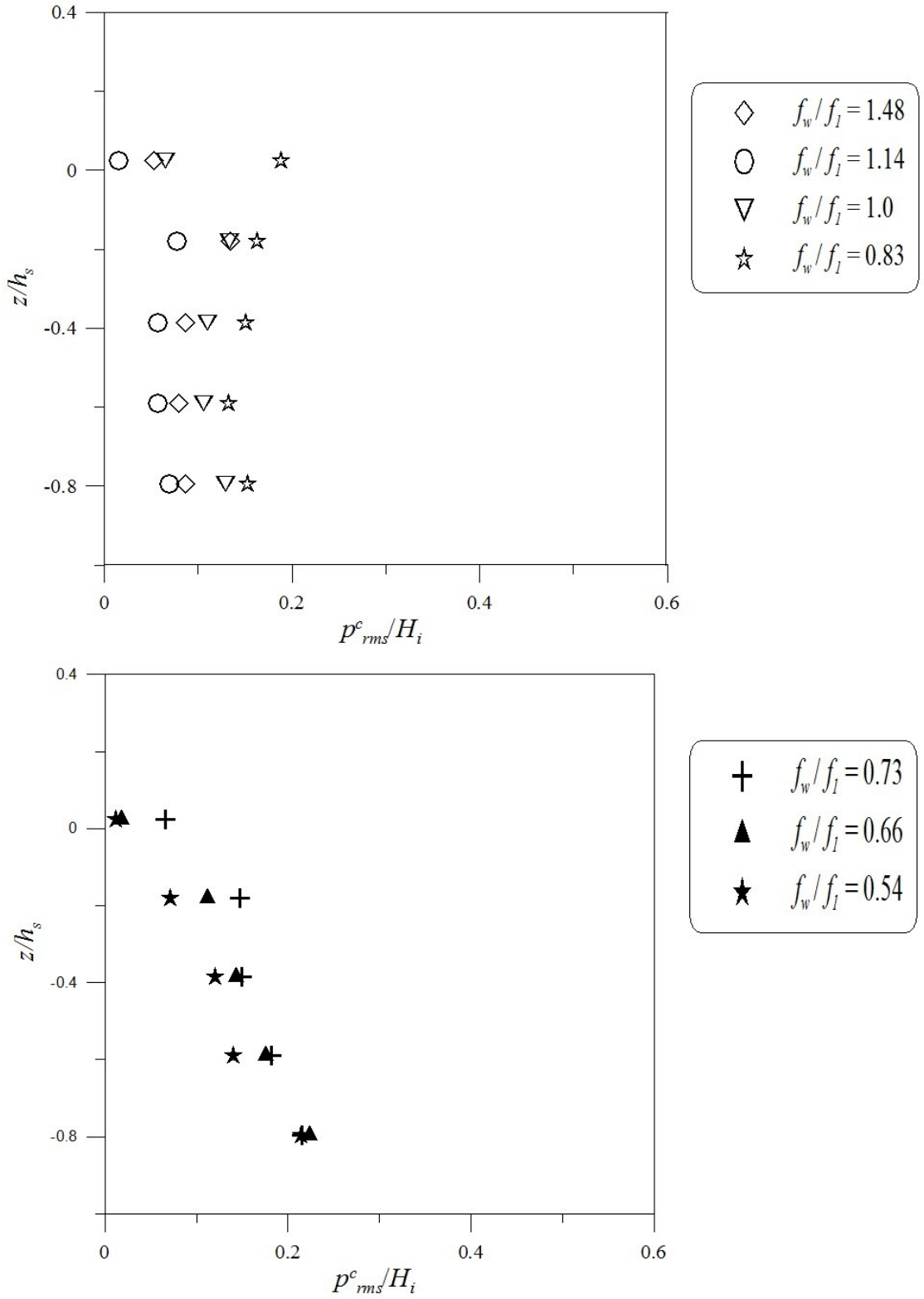

Fig. 21: Variation of p_c^{rms}/H_i at vertical wall (z/h_s) with f_w/f_1 for H_i/d=0.10 and h_s/l=0.488 (Baffle of porosity = 20.2% and placed at *l/3* and *2l/3*)

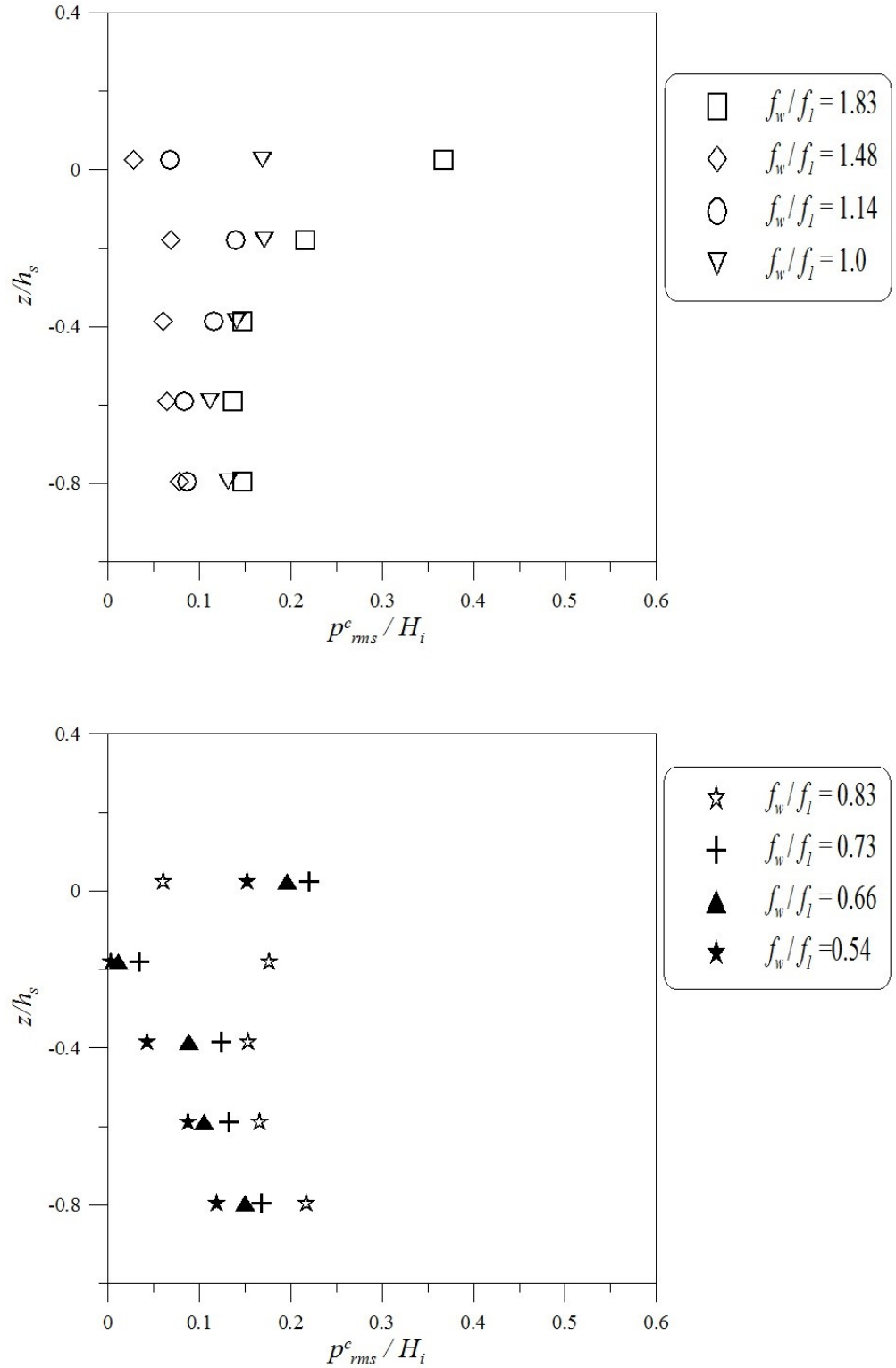

Fig. 22: Variation of p_c^{rms}/H_i at vertical wall (z/h_s) with f_w/f_1 for H_i/d=0.10 and h_s/l=0.488 (Baffle of porosity = 25.2% and placed at $l/3$ and $2l/3$)

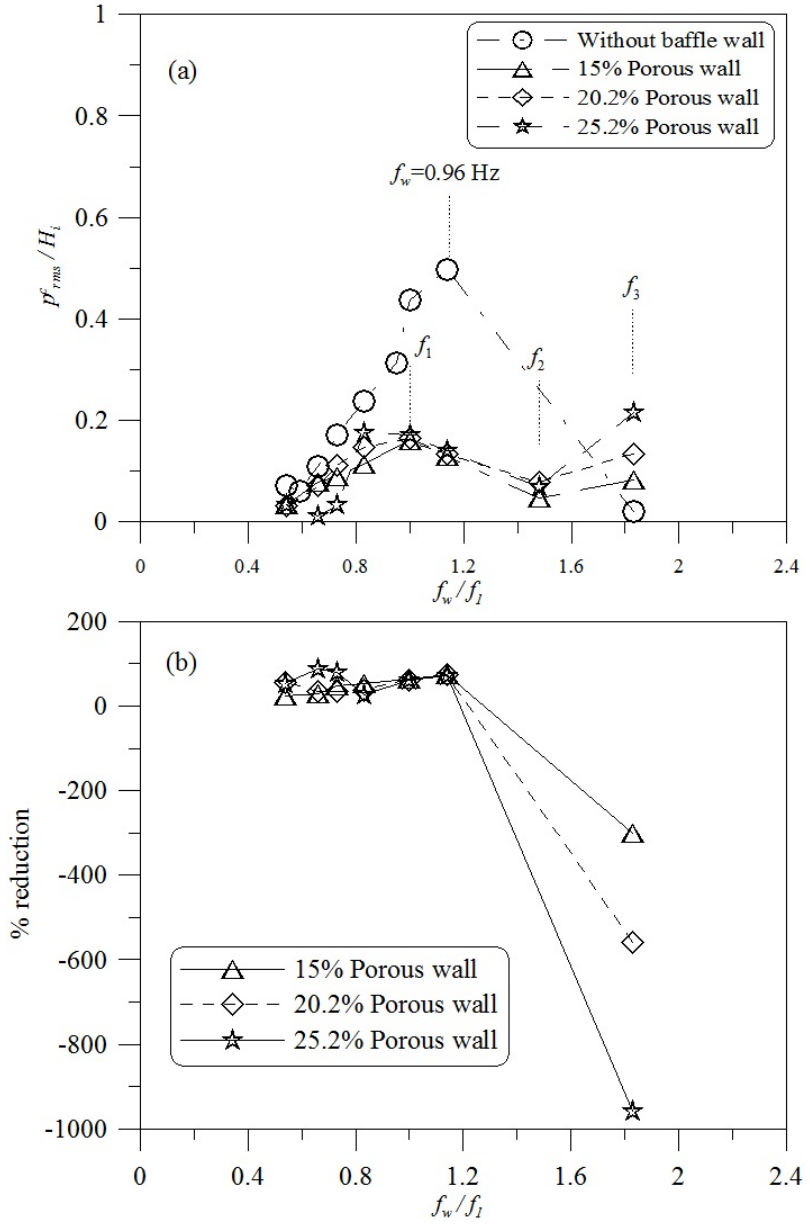

Fig. 23: Variation of (a) p_c^{rms}/H_i and (b) percentage of reduction at P4 with f_w/f_1 for H_i/d=0.10 and h_s/l=0.488 (Baffle placed at l/3 and 2l/3)

It is to be mentioned that the baffle with 20.2% and 25.2% porosities reduces the sloshing pressures, p^c_{rms} and p^c_{max} by an amount of 70% at wave frequency of 0.96 *Hz* (f_w/f_1=1.14). The said reduction in pressure responses is observed to be about 60% at wave excitation of $f_w = f_1$ *Hz* for both the porous conditions. For porosity of 20.2% and by varying the frequency ratio from 0.86 to 0.66, the p^c_{rms} reduces by an average of 35%. However, a reduction of 54% is observed at f_w/f_1 of 0.54. As the frequency ratio decreases between 0.83 and 0.54, the average reduction in p^c_{max} is observed to be about 36%. The dissipation in sloshing pressure, p^c_{rms} tendered by baffle wall of 25.2% porosity for the excitation frequencies ratio of 0.83, 0.73, 0.66, and 0.54 are about 26%, 80%, 89% and 54%, respectively. The said dissipation in p^c_{max} is about 29%, 63%, 31% and 76%, respectively. Similar to 15% porous condition, the baffles with porosities of 20.2% and 25.2% increase p^c_{max} (Fig. 24b) by 113% and 135%, respectively at wave excitation, $f_w = f_3$ *Hz*. Further, the sloshing pressure response, p^c_{rms} is observed to be about 5.5 and 9 times of pressure response (Fig. 23b) observed using un-baffled condition for the baffle with porosities of 20.2% and 25.2%, respectively. This is due to the fact that excitation ratio (f_w/f_1, $f_w = f_3$)

of 1.82 is closer to primary resonance of third mode (f_3/f_1 = 1.73) frequency in solid baffles placed at l/3 and 2l/3 which lead to higher participation of third mode than unbaffled condition (Refer Table 1) and resulting higher sloshing oscillation.

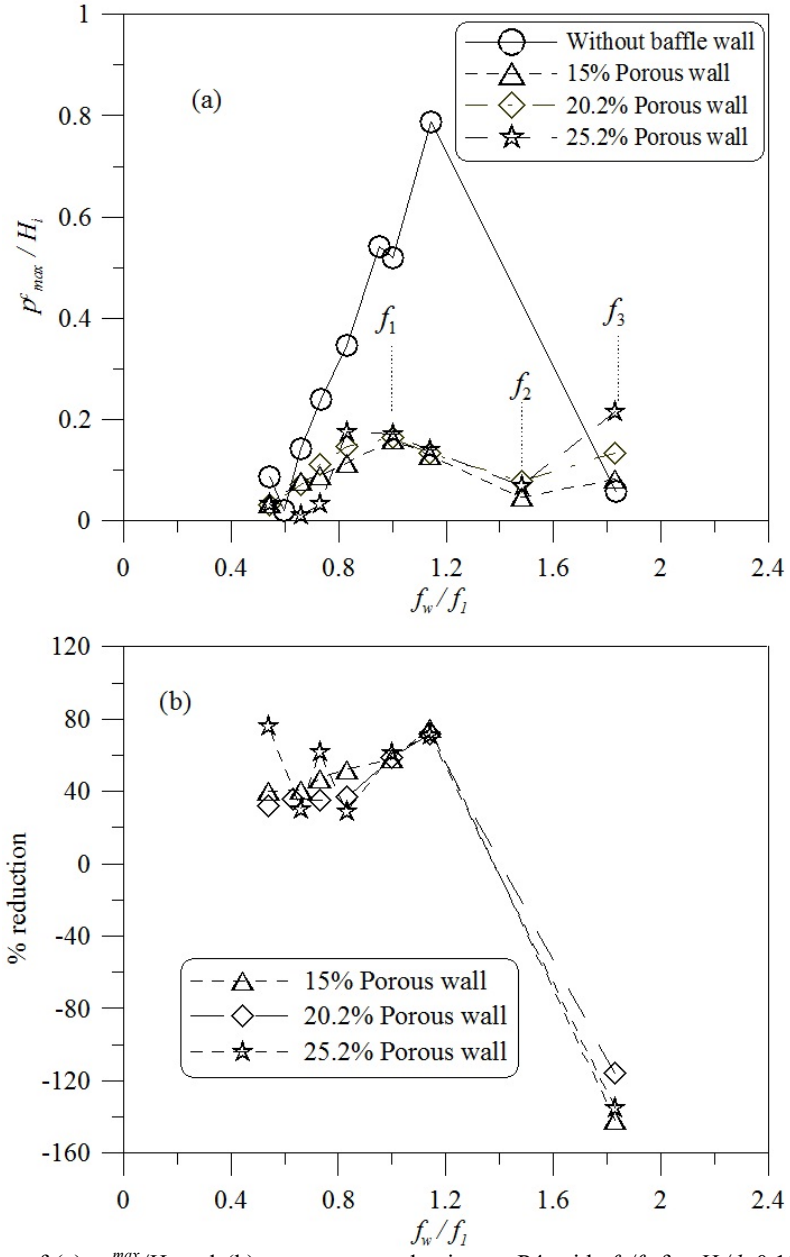

Fig. 24: Variation of (a) p_c^{max}/H_i and (b) percentage reduction at P4 with f_w/f_1 for H_i/d=0.10 and h_s/l=0.488 (Baffle placed at l/3 and 2l/3)

3.2.5 Different baffle wall configurations

To arrive at the best baffle wall configuration in reducing sloshing motion and consequent sloshing pressure, an inter-comparison is made among porous baffle placements. Further, to substantiate the effectiveness of porous baffle, experiment is also conducted (Nasar *et al*., 2018) for a submerged (h_b=h/2) solid baffle placed at center of the tank (l/2). The pressure variation at pressure port location, P4 is compared for the different placements of baffle with individual porosity.

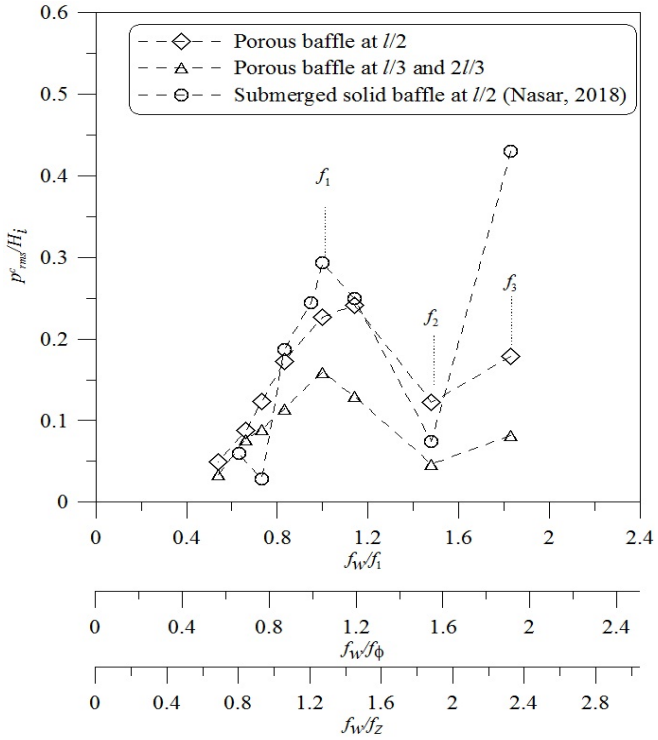

Fig. 25: Variation of p_c^{rms}/H_i at P4 with f_w/f_1 for H_i/d=0.10 and h_s/l=0.488 for 15% porous baffle

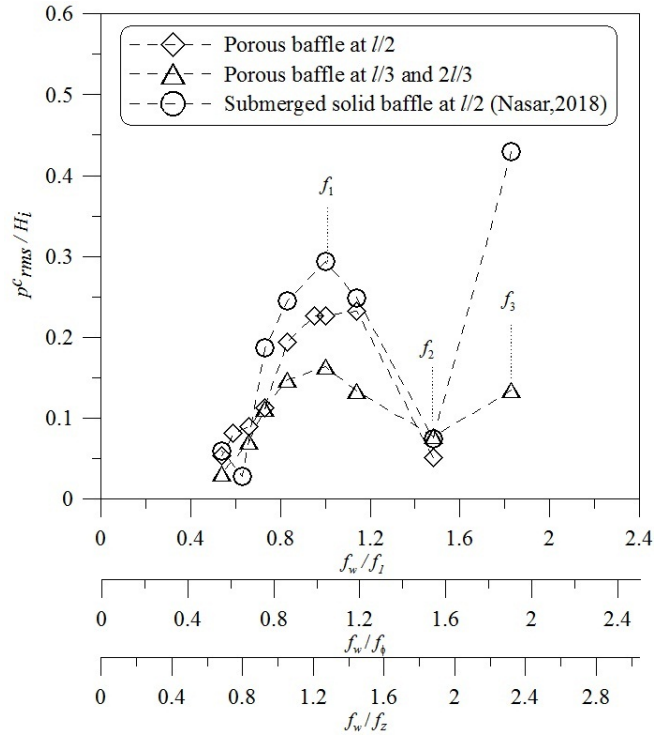

Fig. 26: Variation of p_c^{rms}/H_i at P4 with f_w/f_1 for H_i/d=0.10 and h_s/l=0.488 for 20.2% porous baffle

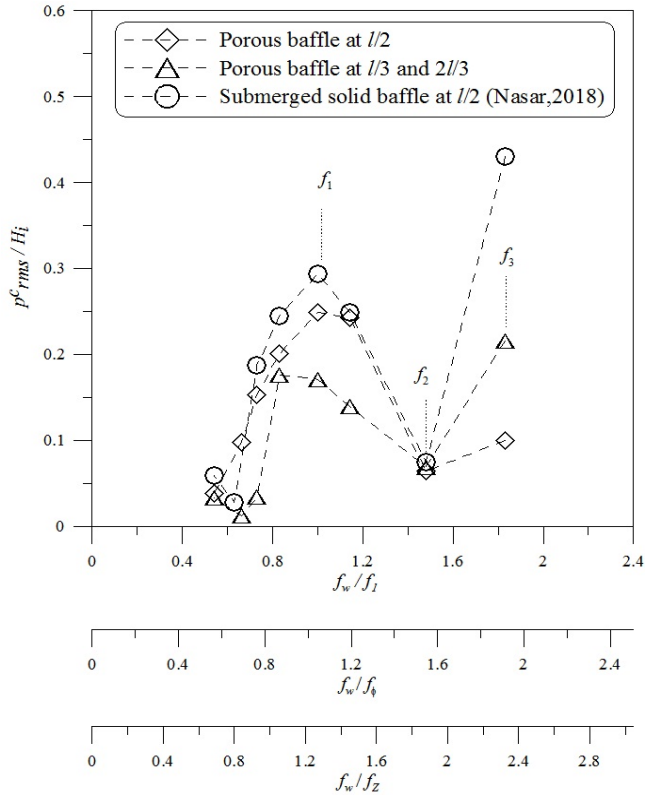

Fig. 27: Variation of p_c^{rms}/H_i at P4 with f_w/f_1 for H_i/d=0.10 and h_s/l=0.488 for 25.2% porous baffle

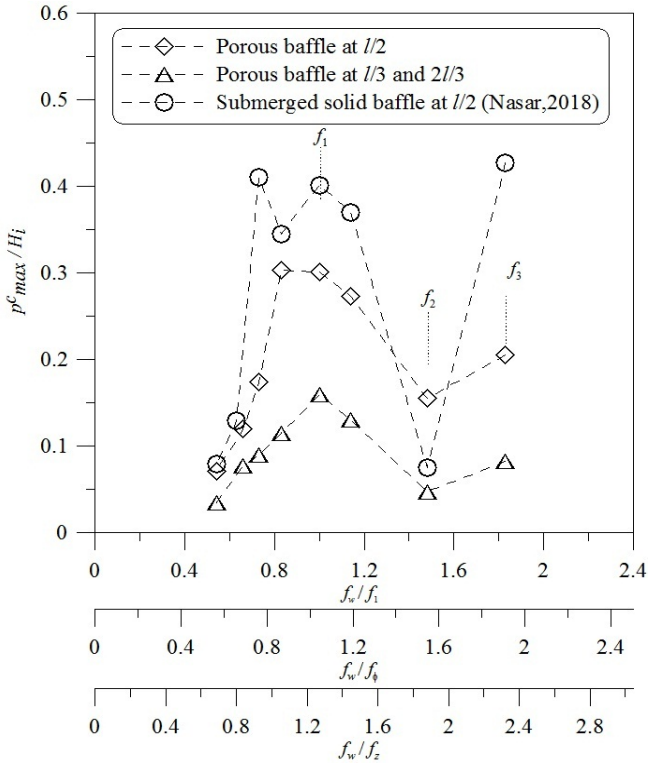

Fig. 28: Variation of p_c^{max}/H_i at P4 with f_w/f_1 for H_i/d=0.10 and h_s/l=0.488 for 15% porous baffle

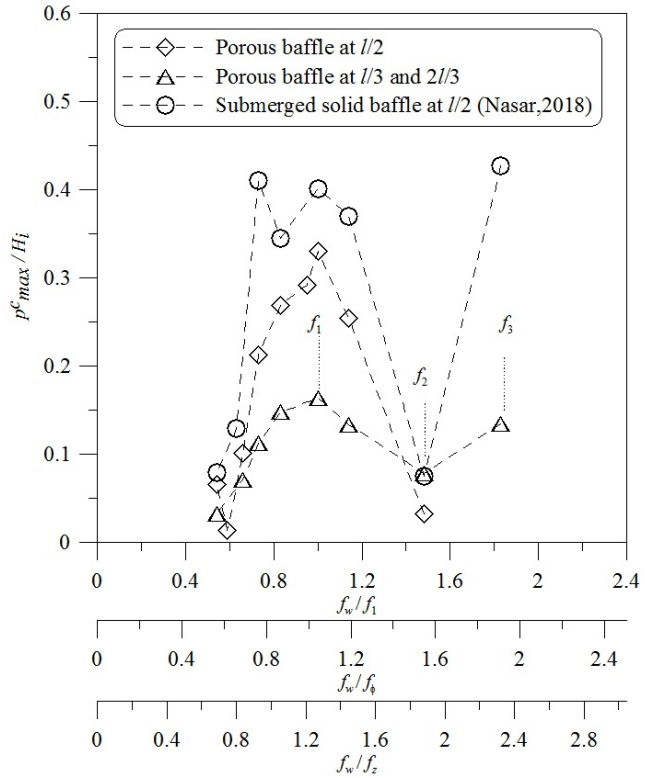

Fig. 29: Variation of p_c^{max}/H_i at P4 with f_w/f_1 for H_i/d=0.10 and h_s/l=0.488 for 20.2% porous baffle

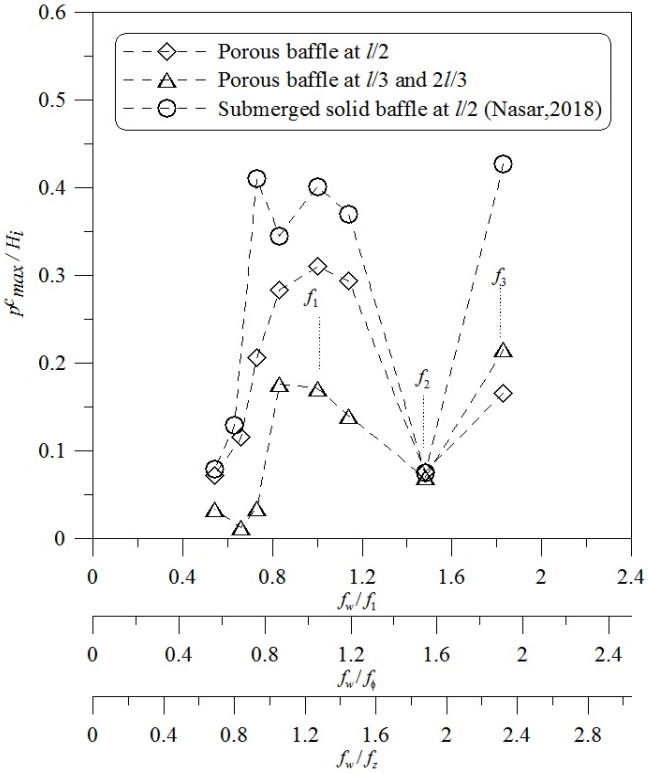

Fig. 30: Variation of p_c^{max}/H_i at P4 with f_w/f_1 for H_i/d=0.10 and h_s/l=0.488 for 25.2% porous baffle

Fig. 25, Fig. 26 and Fig. 27 are depicting the variation of pressure responses for 15%, 20.2% and 25.2% porosities, respectively. It can be noticed that the *rms* pressure (p^c_{rms}) reduction is maximum for baffle wall placed at $l/3$ and $2l/3$ over a wide range of excitation ratios (f_w/f_1) from 0.54 to 1.83 for all the porosities considered. Similar performance is evident for wide range of frequencies ratio in *max* pressure responses (p^c_{max}) as well (Fig. 28, Fig. 29 and Fig. 30). At $f_w = f_3$, all the configurations show their inability in reducing sloshing pressure. Also, submerged solid baffle placed at $l/2$ gives least performance among the baffle wall configurations considered.

4. Conclusions

The present experimental study is focused on exploring the effect of baffles on induced sloshing pressure in a 75% liquid filled tank equipped inside a freely floating barge subjected to beam sea excitations which involve combined sway, heave and roll motions. A wide range of wave excitation frequencies ranging from 0.46 to 1.54 *Hz* (covers upto third mode sloshing frequency) and $H_i/d = 0.1$ is adopted. The effectiveness of porous baffles with porosities 15%, 20.2% and 25% and their placement at different locations such as one baffle at $l/2$ and two baffles at $l/3$ and $2l/3$ are explored on comparison with unbaffled condition and a submerged solid baffle at $l/2$ is explored. The conclusions drawn from the present experimental work are follows:

- A parabolic variation in sloshing pressure distribution is observed across the depth of tank in unbaffled condition.
- On usage of baffles, the impact of liquid observed on tank ceiling is completely avoided on comparison with unbaffled condition for the wave excitation closer to first mode sloshing frequency.
- It is observed that 15% porous baffle is very effective over the wide range of frequencies tested for the baffle placed at $l/2$ position. However, 20.2% porosity is effective for the baffle wall placed at $l/3$ and $2l/3$ locations.
- Porous baffles placed at $l/3$ and $2l/3$ is better in reducing the sloshing compared to porous baffle place at $l/2$ configuration for the wide range of frequencies considered.
- Porous baffles with two different placement configurations are effective in reducing the sloshing pressure compared to submerged solid baffle at $l/2$ for the wide range of frequencies considered.
- It is noticed that all the baffle configurations are not effective in reducing the sloshing pressure for wave excitation frequency ratio of 1.83 which corresponds to third mode of sloshing frequency. This is due to the fulfillment of resonance conditions corresponding to solid baffles which divide the sloshing tank into two equal parts and divide the tank into three equal parts.
- It is understood that barge natural frequencies do not have any influence on sloshing pressure unless the barge frequencies (heave and roll) are closer to the first mode sloshing frequency.

References

Akyildiz, H. and Unal, E. (2005): Experimental investigation of pressure distribution on a rectangular tank due to the liquid sloshing. Ocean Engineering, 32(11–12), 1503–1516. https://doi.org/10.1016/j.oceaneng.2004.11.006.

Akyildiz, H. and Unal, E. (2006): Sloshing in a three dimensional rectangular tank: numerical simulation and experimental validation. Ocean engineering, 33(16), 2135-2149. https://doi.org/10.1016/j.oceaneng.2005.11.001

Akyildiz, H. (2012): A numerical study of the effects of the vertical baffle on liquid sloshing in two-dimensional rectangular tank. Journal of Sound and Vibration, 331(1), 41–52. https://doi.org/10.1016/j.jsv.2011.08.002.

Armenio, V. and La Rocca, M. (1996): On the analysis of sloshing of water in rectangular containers: Numerical study and experimental validation. Ocean Engineering, 23(8), 705–739. https://doi.org/10.1016/0029-8018(96)84409-X.

Bulian, G., Botia-Vera, E. and Souto-Iglesias, A. (2014): Experimental sloshing pressure impacts in ensemble domain: Transient and stationary statistical characteristics. Physics of Fluids, 26(3). https://doi.org/10.1063/1.4866315.

Bunnik, T. and Huijsmans, R. (2007): Large scale sloshing model tests. Proceedings of the Seventeenth International Offshore and Polar Engineering Conference, Lisbon, Portugal, July, 1893-1899.

Cariou, A. and Casella, G. (1999): Liquid sloshing in ship tanks: A comparative study of numerical simulation. Marine Structures, 12(3), 183–198. https://doi.org/10.1016/S0951-8339(99)00026-X.

Celebi, M. S. and Akyildiz, H. (2002): Nonlinear modeling of liquid sloshing in a moving rectangular tank. Ocean Engineering, 29(12), 1527–1553. https://doi.org/10.1016/S0029-8018(01)00085-3

Chen, B.F. and Chiang, H.W. (2000): Complete two dimensional analysis of sea wave induced fully nonlinear sloshing fluid in a rigid floating tank. Ocean Engineering, 27, 953-977.

Chu, C. R., Wu, Y. R., Wu, T. R. and Wanga, C. Y. (2018): Slosh-induced hydrodynamic force in a water tank with multiple baffles. Ocean Engineering, 167, 282–292. https://doi.org/10.1016/j.oceaneng.2018.08.049.

Cho, I. H., Choi, J. and Kim, M. H. (2017): Sloshing reduction in a swaying rectangular tank by an horizontal porous baffle. Ocean Engineering, 138, 23–34. https://doi.org/10.1016/j.oceaneng.2017.04.005.

Crowley, S and Porter, R. (2012): An analysis of screen arrangements for a tuned liquid damper. Journal of Fluids and Structures, 34, 291–309.

Faltinsen, O. M. and Timokha, A. N. (2001): An adaptive multimodal approach to nonlinear sloshing in a rectangular tank. Journal of Fluid Mechanics, 432, 167–200.

Francescutto, A. and Contento, G. (1994): An experimental study of the coupling between roll motion and sloshing in a compartment. Proceedings of the Fourth International Offshore and Polar Engineering Conference, Osaka, Japan, April, 10-15.

Francescutto, A. and Contento, G. (1999): An investigation of simplified mathematical models to the roll-sloshing problem. Proceedings of the International Journal of Offshore and Polar Engineering, 9(2), 97-104.

Graczyk, M., Moan, T. and Rognebakke, O. (2006): Probabilistic analysis of characteristic pressure for LNG Tanks. Journal of Offshore Mechanics and Arctic Engineering, 128(2), 133. https://doi.org/10.1115/1.2185128.

Ibrahim, R.A. (2005): Liquid Sloshing Dynamics - Theory and Applications, Cambridge University press, Newyork.

Iranmanesh, A. (2017): A 2D numerical study on suppressing liquid sloshing using a submerged cylinder. Ocean Engineering, 138, 55–72. https://doi.org/10.1016/j.oceaneng.2017.04.022.

Kim, Y. (2001): Numerical simulation of sloshing flows with impact load. Applied Ocean Research, 23(1), 53–62. https://doi.org/10.1016/S0141-1187(00)00021-3.

Kim, Y., Shin, Y., Kim, W. and Yue, D. (2003): Study on sloshing problem coupled with ship motion in waves. Proceedings of the eigth international conference on Numerical Ship Hydrodynamics, Busan, Korea.

Kim, Y., Nam, B. W., Kim, D. W. and Kim, Y. S. (2007): Study on coupling effects of ship motion and sloshing. Ocean Engineering, 34(16), 2176–2187. https://doi.org/10.1016/j.oceaneng.2007.03.008.

Lee, D.H., Kim, M.H., Kwon, S.H., Kim, J.W. and Lee, Y.B. (2005): A parametric and numerical study on LNG-tank sloshing loads. Proceedings of the fifteenth International Offshore and Polar engineering Conference, Seoul, Korea, June, 228-232.

Lee, S. J., Kim, M. H., Lee, D. H., Kim, J. W. and Kim, Y. H. (2007): The effects of LNG-tank sloshing on the global motions of LNG carriers, 34, 10–20. https://doi.org/10.1016/j.oceaneng.2006.02.007.

Lu, L., Jiang, S. C., Zhao, M., and Tang, G. Q. (2015): Two-dimensional viscous numerical simulation of liquid sloshing in rectangular tank with/without baffles and comparison with potential flow solutions. Ocean Engineering, 108, 662–677. https://doi.org/10.1016/j.oceaneng.2015.08.060.

Mikelis, N.E. and Journee J.M.J. (1984): Experimental and numerical simulation of sloshing behaviour in liquid cargo tanks and its effect on ship motions, Delft University of Technology, Report 0661-P, Ship hydrodynamics laboratory.

Modi and Munshi. (1998): An efficient liquid sloshing damper for vibration control, Journal of Fluids and Structures, 12(8), 1055–1071.

Modi, V. J. and Akinturk, A. (2002):An efficient liquid sloshing damper for control of wind-induced instabilities, Journal of Wind Engineering and Industrial Aerodynamics, 90, 1907–1918.

Molin, B., Remy, F., Rigaud, S. and Ch. de Jouette. (2002): LNG-FPSO's: Frequency domain coupled analysis of support and liquid cargo motion. Proceedings of the IMAM Conference, Rethymnon, Greece.

Molin, B. and Remy, F. (2013): Experimental and numerical study of the sloshing motion in a rectangular tank with a perforated screen, Journal of Fluids and Structures, 43, 463–480. doi: 10.1016/j.jfluidstructs.2013.10.001

Morsy H, Marivani M and Hamed. (2008): Effect of a tuned liquid damper screen configuration on structure response. Proceedings of the Nineth International Congress of Fluid Dynamics & Propulsion – ASME, Alexandria, Egypt.

Nakayama, T. and Washizu, K. (1980):Nonlinear analysis of liquid motion in a container subjected to forced pitching oscillation. International Journal for Numerical Methods in Engineering, 15(8), 1207–1220. https://doi.org/10.1002/nme.1620150808

Nasar, T., Sannasiraj, S. A. and Sundar, V. (2008): Sloshing pressure variation in a barge carrying tank. Ships and Offshore Structures, 40(6), 185–203. https://doi.org/10.1016/j.fluiddyn.2008.02.001

Nasar, T., Sannasiraj, S. A. and Sundar, V. (2010): Motion responses of barge carrying liquid tank. Ocean Engineering, 37(10), 935–946. https://doi.org/10.1016/j.oceaneng.2010.03.006

Nasar, T., Sannasiraj, S. A. and Sundar, V. (2009): Wave-induced sloshing pressure in a liquid tank under irregular waves. Proceedings of the Institution of Mechanical Engineers, Part M: Journal of Engineering for the Maritime Environment, 223(2), 145–161. https://doi.org/10.1243/14750902JEME135.

Nasar, T. and Sannasiraj, S. A. (2018): Experimental investigation on effect of submerged solid baffle in a barge carrying liquid sloshing tank in the book titled "Lecture Notes in Civil Engineering," edited by Murali K., Sriram V., Samad A., Saha N. (eds.) Springer, Singapore, 22, 365-384.

Nielsen, K. B. and Mayer, S. (2004): Numerical prediction of green water incidents. Ocean Engineering, 31(3–4), 363–399. https://doi.org/10.1016/j.oceaneng.2003.06.001

Ockendon, H., Ockendon, J. R. and Johnson, A. D. (1986): Resonant sloshing in shallow water. Journal of Fluid Mechanics, 167(1), 465. https://doi.org/10.1017/S0022112086002926

Paik, J. K. and Shin, Y. S. (2006): Structural damage and strength criteria for ship stiffened panels under impact pressure actions arising from sloshing, slamming and green water loading. Ships and Offshore Structures, 1(3), 249-256. https://doi.org/10.1533/saos.2006.0109

Panigrahy, P. K., Saha, U. K. and Maity, D. (2009): Experimental studies on sloshing behavior due to horizontal movement of liquids in baffled tanks. Ocean Engineering, 36(3–4), 213–222. https://doi.org/10.1016/j.oceaneng.2008.11.002

Rognebakke, O. R. and Faltinsen, O. M. (2001): Effects of sloshing on ship motions. Proceedings of the 16th Workshop on Water Waves and Floating Bodies, Hiroshima, Japan.

Saghi, H. (2016): The pressure distribution on the rectangular and trapezoidal storage tanks perimeters due to liquid sloshing phenomenon. International Journal of Naval Architecture and Ocean Engineering, 8(2), 153–168. https://doi.org/10.1016/j.ijnaoe.2015.12.001

Sannasiraj, S.A., Sundar V. and Sundaravadivelu, R. (1995): The hydrodynamic behaviour of long floating structures in directional seas. Applied Ocean Research, **17**, 233-243.

Kim, S. P., Chung, S. M., Shin, W. J., Cho, D. S. and Park, J. C. (2018): Experimental study on sloshing reduction effects of baffles linked to a spring system. Ocean Engineering, 170, 136–147. https://doi.org/10.1016/j.oceaneng.2018.10.001.

Tait, M. J., Damatty, El Isyumov, A. A., Isyumov, N. and Siddique, M. R. (2005): Numerical flow models to simulate tuned liquid dampers (TLD) with slat screens. Journal of Fluids and Structures, 20, 1007–1023. https://doi.org/10.1016/j.jfluidstructs.2005.04.004

Virella, J. C., Prato, C. A. and Godoy, L. A. (2008): Linear and nonlinear 2D finite element analysis of sloshing modes and pressures in rectangular tanks subject to horizontal harmonic motions. Journal of Sound and Vibration, 312(3), 442–460. https://doi.org/10.1016/j.jsv.2007.07.088

Warnitchai, P. and Pinkaew, T. (1998): Modelling of liquid sloshing in rectangular tanks with flow-dampening devices. Engineering Structures, 20(97), 593–600. https://doi.org/10.1016/S0141-0296(97)00068-0

Xue, M. A., Zheng, J. and Lin, P. (2012): Numerical simulation of sloshing phenomena in cubic tank with multiple baffles. Journal of Applied Mathematics, Vol.2012. https://doi.org/10.1155/2012/245702

Xue, M., Zheng, J., Lin, P. and Yuan, X. (2017): Experimental study on vertical baffles of different configurations in suppressing sloshing pressure, 136, 178–189. https://doi.org/10.1016/j.oceaneng.2017.03.031